Auckland
Regional Council
TE RAUHĪTANGA TAIAO

Southeastern Manukau / Pahurehure Inlet Contaminant Study: Hydrodynamic, Wave and Sediment-Transport Model Implementation and Calibration
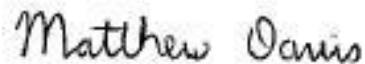
December   TR 2008/056

Technical Report. First Edition.

Reviewed by: Approved for ARC Publication by:

Name: Judy-Ann Ansen

Position: Acting Team Leader
Stormwater Action Team

Organisation: Auckland Regional Council

Date: 28 October 2010

Name: Matthew Davis

Position: Group Manager
Partnerships & Community Programmes

Organisation: Auckland Regional Council

Date: 28 October 2010

Southeastern Manukau / Pahurehure Inlet Contaminant Study: Hydrodynamic, Wave and Sediment-Transport Model Implementation and Calibration

Mark Pritchard
Richard Gorman
Matt Lewis

Reviewed by:

Scott Stephens

Approved for release by:

Andrew Swales

PREFACE

The Manukau Harbour is comprised of tidal creeks, embayments and the central basin. The harbour receives sediment and stormwater chemical contaminant run-off from urban and rural land from a number of subcatchments, which can adversely affect the ecology. State of the environment monitoring in the Pahurehure Inlet showed increasing levels of sediment and stormwater chemical contaminant build up. However, previously little was known about the expected long-term accumulation of sediment and stormwater chemical contaminants in the inlet or adjacent portion of the Manukau Harbour. The South Eastern Manukau Harbour / Pahurehure Inlet Contaminant Study was commissioned to improve understanding of these issues. This study is part of the 10-year Stormwater Action Plan to increase knowledge and improve stormwater management outcomes in the region. The work was undertaken by the National Institute of Water and Atmospheric Research (NIWA).

The scope of the study entailed:

1. field investigation,

2. development of a suite of computer models for

   a. urban and rural catchment sediment and chemical contaminant loads,

   b. harbour hydrodynamics, and

   c. harbour sediment and contaminant dispersion and accumulation,

3. application of the suite of computer models to project the likely fate of sediment, copper and zinc discharged into the central harbour over the 100-year period 2001 to 2100, and

4. conversion of the suite of computer models into a desktop tool that can be readily used to further assess the effects of different stormwater management interventions on sediment and stormwater chemical contaminant accumulation in the central harbour over the 100-year period.

The study is limited to assessment of long-term accumulation of sediment, copper and zinc in large-scale harbour depositional zones. The potential for adverse ecological effects from copper and zinc in the harbour sediments was assessed against sediment quality guidelines for chemical contaminants.

The study and tools developed address large-scale and long timeframes and consequently cannot be used to assess changes and impacts from small subcatchments or landuse developments, for example. Furthermore, the study does not assess ecological effects of discrete storm events or long-term chronic or sub-lethal ecological effects arising from the cocktail of urban contaminants and sediment.

The range of factors and contaminants influencing the ecology means that adverse ecological effects may occur at levels below contaminant guideline values for individual

chemical contaminants (i.e., additive effects due to exposure to multiple contaminants may be occurring).

Existing data and data collected for the study were used to calibrate the individual computer models. The combined suite of models was calibrated against historic sediment and copper and zinc accumulation rates, derived from sediment cores collected from the harbour.

Four scenarios were modelled: a baseline scenario and three general stormwater management intervention scenarios.

The baseline scenario assumed current projections (at the time of the study) of

- future population growth,

- future landuse changes,

- expected changes in building roof materials,

- projected vehicle use, and

- existing stormwater treatment.

The three general stormwater management intervention scenarios evaluated were:

1. source control of zinc from industrial areas by painting existing unpainted and poorly painted galvanised steel industrial building roofs;
2. additional stormwater treatment, including:

  - raingardens on roads carrying more than 20,000 vehicles per day and on paved industrial sites,

  - silt fences and hay bales for residential infill building sites and

  - pond / wetland trains treating twenty per cent of catchment area; and
3. combinations of the two previous scenarios.

International Peer Review Panel
The study was subject to internal officer and international peer review. The review was undertaken in stages during the study, which allowed incorporation of feedback and completion of a robust study. The review found:

- a state-of-the-art study on par with similar international studies,

- uncertainties that remain about the sediment and contaminant dynamics within tidal creeks / estuaries, and

- inherent uncertainties when projecting out 100 years.

Key Findings of the Study

Several key findings can be ascertained from the results and consideration of the study within the context of the wider Stormwater Action Plan aim to improve stormwater outcomes:

- The inner tidal creeks and estuary branches of the Pahurehure Inlet continue to accumulate sediment and contaminants, in particular in the eastern estuary of Pahurehure Inlet (east of the motorway).

- The outer Pahurehure Inlet/Southeastern Manukau bed sediment concentrations of copper and zinc are not expected to reach toxic levels based on current assumptions of future trends in landuse and activities.

- Zinc source control targeting industrial building roofs produced limited reduction of zinc accumulation rates in the harbour because industrial areas cover only a small proportion of the catchment area and most unpainted galvanised steel roofs are expected to be replaced with other materials within the next 25 to 50 years.

- Given that the modelling approach used large-scale depositional zones and long timeframes, differences can be expected from the modelling projections and stormwater management interventions contained within these reports versus consideration of smaller depositional areas and local interventions. As a consequence, these local situations may merit further investigation and assessment to determine the best manner in which to intervene and make improvements in the short and long terms.

Research and Investigation Questions

From consideration of the study and results, the following issues have been identified that require further research and investigation:

- Sediment and chemical contaminant dynamics within tidal creeks.

- The magnitude and particular locations of stormwater management interventions required to arrest sediment, copper and zinc accumulation in tidal creeks and embayments, including possible remediation / restoration opportunities.

- The fate of other contaminants derived from urban sources.

- The chronic / sub-lethal effects of marine animal exposure to the cocktail of urban contaminants and other stressors such sediment deposition, changing sediment particle size distribution and elevated suspended sediment loads.

- Ecosystem health and connectivity issues between tidal creeks and the central basin of the harbour, and the wider Manukau Harbour.

Technical reports

The study has produced a series of technical reports:

Technical Report TR2008/049
Southeastern Manukau Harbour / Pahurehure Inlet Harbour Contaminant Study.
Landuse Analysis.

Technical Report TR2008/050
Southeastern Manukau Harbour / Pahurehure Inlet Contaminant Study. Sediment
Load Model Structure, Setup and Input Data.

Technical Report TR2008/051
Southeastern Manukau Harbour / Pahurehure Inlet Contaminant Study. Sediment
Load Model Evaluation.

Technical Report TR2008/052
Southeastern Manukau Harbour / Pahurehure Inlet Contaminant Study. Sediment
Load Model Results.

Technical Report TR2008/053
Southeastern Manukau Harbour / Pahurehure Inlet Contaminant Study. Predictions
of Stormwater Contaminant Loads.

Technical Report TR2008/054
Southeastern Manukau Harbour / Pahurehure Inlet Contaminant Study. Harbour
Sediments.

Technical Report TR2008/055
Southeastern Manukau Harbour / Pahurehure Inlet Contaminant Study. Harbour
Hydrodynamics and Sediment Transport Fieldwork.

Technical Report TR2008/056
Southeastern Manukau Harbour / Pahurehure Inlet Contaminant Study.
Hydrodynamic Wave and Sediment Transport Model Implementation and Calibration.

Technical Report TR2008/057
Southeastern Manukau Harbour / Pahurehure Inlet Contaminant Study.
Implementation and Calibration of the USC-3 Model.

Technical Report TR2008/058
Southeastern Manukau Harbour / Pahurehure Inlet Contaminant Study. Predictions
of Sediment, Zinc and Copper Accumulation under Future Development Scenario 1.

Technical Report TR2008/059
Southeastern Manukau Harbour / Pahurehure Inlet Contaminant Study. Predictions
of Sediment, Zinc and Copper Accumulation under Future Development Scenarios 2,
3 and 4.

Technical Report TR2009/110
Southeastern Manukau Harbour / Pahurehure Inlet Contaminant Study. Rainfall
Analysis.

Southeastern Manukau Harbour/Pahurehure Inlet Contaminant Study:
Hydrodynamic wave and sediment transport model implementation and calibration

4

Contents

1 Executive Summary

The main aim of the Southeastern Manukau Harbour / Pahurehure Inlet Contaminant Study is to model contaminant (zinc, copper) and sediment accumulation for the purposes of, amongst other things, identifying significant contaminant sources, and testing efficacy of stormwater treatment options.

This report addresses the implementation and calibration of three models used in the study: an estuarine hydrodynamic model, a wave model, and a sediment-transport model. Together these simulated the dispersal of contaminants and sediments by physical processes such as tidal currents and waves.

The models used in the study were the DHI Water and Environment MIKE3 FM HD hydrodynamic model, the DHI MIKE3 FM MT (mud) sediment transport model, and the SWAN wave model.

The new Southeastern Manukau and Pahurehure model bathymetric mesh was produced from a combination of a previously calibrated 2-dimensional model mesh and further updated bathymetry from LIDAR surveys supplied by the Auckland Regional Council (ARC). This provided extra information on the intertidal mud flats and in the tidal creeks.

The implementation and calibration of the MIKE3 model was based on two field data sets collected between February and May 2007. These time series of observed water levels, currents, suspended sediment and wave statistics were used to calibrate the model(s).

The calibrated hydrodynamic model provided good predictions of water surface elevations and semi-diurnal tidal currents. However, the model was sensitive to the model grid which caused some deviations of predicted currents from those observed at some specific mooring sites in the inner harbour where bathymetric sounding data was scarce. Wind driven currents and waves in the enclosed region of the Pahurehure were small. Predicted wave heights from the SWAN model agreed well with measurements.

The model provided a reasonable estimate of salinity around the Southeastern Harbour and Pahurehure Inlet. This is important for predicting dispersal of catchment-derived sediments and contaminants delivered to the harbour in freshwater runoff. However, the lack of rainfall during two field programs meant that the salinity calibration was restricted to baseflow freshwater input conditions.

Measurements of suspended sediment concentration from several sites were used to calibrate the MIKE3 MT sediment transport model. The resuspension and transport of three constituent grainsizes (4, 12 and 40 μm) were simulated. The constituent concentrations were combined to yield a total concentration, which was then compared to measurements. The calibrated model was able to satisfactorily reproduce the phase and magnitude of suspended sediment concentration under multiple tide cycles, under weak winds and small locally generated waves. However, the model was deficient in simulating some of the inherent variability of the region. The MIKE3 MT model was properly constituted for the 4 and 12 μm fractions, but not necessarily for the 40 μm fraction. Nevertheless, with the exception of narrow tidal creeks, the 40 μm concentrations predicted by the model were in agreement with a non-cohesive

Southeastern Manukau Harbour/Pahurehure Inlet Contaminant Study:
Hydrodynamic wave and sediment transport model implementation and calibration

7

reference-concentration model more normally applied to silt-sand size fractions. Furthermore, the 40 µm fraction constituted only a small fraction of the predicted total suspended-sediment load.

2   Introduction

Empirical data and modelling simulations indicate that stormwater contaminants are rapidly accumulating in the Southeastern Manukau Harbour and Pahurehure Inlet. Stormwater contaminants, which include zinc and copper, are discharged to the Pahurehure Inlet with runoff derived from mainly urban and industrial catchments. This problem, induced by surrounding urbanisation and industrialisation may be further compounded by ongoing and future developments in the surrounding areas. To date there is no clear understanding of the fate of contaminants exported from numerous creeks and side-branches into the main body of the inlet and harbour, or that of contaminants discharged directly into the harbour.

The main aim of the Southeastern Manukau Harbour / Pahurehure Inlet Contaminant Study is to model contaminant (zinc, copper) and sediment accumulation for the purposes of, amongst other things, identifying significant contaminant sources, and testing efficacy of stormwater treatment options.

2.1   Study aims

2.1.1   The Overall Study aims

- Predict contaminant loads based on past, present and future landuse and population growth for each subcatchment discharging into the SEM, allowing for stormwater treatment and zinc source control of industrial areas.

- Predict dispersal and accumulation (or loss) of sediment and stormwater contaminants in the SEM.

- Calibrate and validate the dispersal/accumulation model.

- Apply the various models to predict catchment contaminant loads and accumulation of copper, zinc and sediment in the SEM under specific scenarios that depict various combinations of projected landuse / population growth, stormwater treatment efficiency, and zinc source control of industrial areas.

- Determine from the model predictions the relative contributions of sediment and contaminant from individual sub-catchments.

- Provide an assessment of the environmental consequences of model outputs.

- Provide technical reports on each component of the work.

- Provide a desktop application suitable for use by ARC personnel.

Specific Aims of this Study

- Provide a calibrated 3-dimensional hydrodynamic, wave and sediment transport model that is capable of simulating the input, transport and deposition of three sediment size fractions in the SEM-Pahurehure Inlet.

- The calibrated models would then be later driven by several different 'weather' scenarios based on freshwater input, winds, waves and tides to determine sediment transport and deposition around the inlet and harbour.

- Use the final model output as an input to the USC-3 model.

2.2   Model suite

The Study centres on the application of a suite of models that are linked to each other:

- The GLEAMS sediment-generation model, which predicts sediment erosion from the land and transport down the stream channel network. Predictions of sediment supply are necessary because, ultimately, sediment eroded from the land dilutes the concentration of contaminants in the bed sediments of the harbour, making them less harmful to biota.

- The Contaminant Load Model (CLM)- a contaminant/sediment-generation model, which predicts sediment and contaminant concentrations (including zinc, copper) in stormwater at a point source, in urban streams, or at end-of-pipe where stormwater discharges into the receiving environment. Note the main distinction between the use of GLEAMS and CLM for estimating sediment generation in this study is that the former is largely used for rural areas and the latter for urban areas. Further details are given in Moores and Timperley (2008).

  The USC-3 (Urban Stormwater Contaminant) contaminant/sediment accumulation model, which predicts sedimentation and accumulation of contaminants (including zinc, copper) in the bed sediments of the estuary. Underlying the USC-3 model is yet another suite of models: the **DHI** Water and Environment **MIKE3 FM HD** hydrodynamic model, the **DHI MIKE3 FM MT** (mud) sediment transport model, and the **SWAN** wave model (Holthuijsen et al. 1993), which simulate harbour hydrodynamics and sediment transport. Combined, these three models can be used to simulate tidal propagation, tide- and wind-driven currents, freshwater mixing, waves, and sediment transport and deposition within a harbour."

2.3   This report

This report documents the implementation, calibration and validation of the harbour and inlet hydrodynamic model, the wave model and the sediment-transport model to meet the requirements of Section 2.3. The particular models used in the study were the: DHI Water and Environment MIKE3 FM HD hydrodynamic model, the DHI MIKE3 FM MT (mud) sediment transport model (http://www.dhigroup.com), and the SWAN wave model (Holthuijsen et al. 1993). Combined, these can be used to simulate tidal

propagation, tide- and wind-driven currents, freshwater mixing, waves, and sediment transport and deposition within a harbour.

These combined model outputs underpin the distribution of harbour and inlet suspended sediment and bed deposition used in the USC model (Section 2.3).

2.3.1   The DHI MIKE3 FM HD and MT Model

The Pahurehure Inlet and Southeastern Manukau harbour was modelled using the DHI MIKE3 FM HD hydrodynamic and MT (mud) sediment transport modelling suite. The finite element, 3-dimensional sigma coordinate (multi-layer) semi-implicit model finds numerical solutions for the Navier-Stokes equations for momentum whilst conserving mass through the principle of continuity. Physical processes in the model can be parameterised / simulated through specifying for example, eddy scales, turbulent closure schemes, surface and bottom boundary conditions, salinity/temperature structure and the earth's rotational effects. The model's open boundary is initialised and forced using tidal data and source inputs of freshwater which allows variation in seawater density to be included in model solutions. The finite element grid and baroclinic capability, plus the inclusion of a wetting and drying scheme, makes the model ideal for simulating time/spatially varying gravity, density and tidally driven flows in coastal regions with complex shoreline and embayments with varying bathymetry.

The MIKE3 FM HD model can be forced at boundaries by both oceanic/estuarine tides and freshwater sources. These two forcing mechanisms effectively produce the essential boundary physics required to simulate barotropic (tides and surface pressure gradients) and baroclinic (internal pressure gradients driven by horizontal and vertical density differences) features in the model domain. The effects of geostrophy, i.e., currents produced by the force balance between pressure gradients and the earth's rotation, are negligible for the size of domain under consideration for this study.

Sediment transport in the MIKE3 FM MT model is simulated through the application of the advection-diffusion (transport) equation. In addition to estuarine dynamics, the effects of localised surface wave fields on sediment erosion, deposition, re-suspension and transport are also computed and included into final model predictions.

Particles of a specified size may be introduced into the model scheme as a sediment flux associated with each specific freshwater discharge into the model domain. The total sediment load can then be split into specific size ranges, each with a specified Stokes settling velocity and critical depositional/erosion shear stress. The modelled estuarine hydrodynamics and application of the advection-diffusion scheme then transport this sediment flux around the model domain.

Localised model morphological evolution is based on deposition and erosion of sediments transported in the model domain i.e., bed levels are updated at each time step. This effectively, through both continuity and dynamical constraints, causes change and feedback in the modelled hydrodynamic and transport equations (see Appendix 2).

2.3.2   The SWAN Wave Model

The SWAN wave model is a spectral wave model particularly suited to shallow-water applications in coastal and estuarine environments. It describes the sea state in terms of the amount of energy associated with each wave frequency and propagation direction. The model computes the evolution of the wave spectrum by accounting for the input, transfer and loss of energy through various physical processes.

In addition to specified wind fields, the SWAN model uses the water levels and current fields predicted by the MIKE3 FM HD model in predicting the wind-generated waves in the MIKE3 FM model domain. The predicted wave heights, periods and directions are in turn used through linear wave theory to quantify wave orbital velocities which produce a wave-induced bed shear stress, which then transports sediments in the MIKE3 FM MT model (see Appendix 2).

3 Study Requirements and Model Development

Delivery of catchment sediment into the wider Southeastern Manukau Harbour and Pahurehure Inlet is very dependent on tidal creek dynamics. Therefore, these narrow channels required a more refined model mesh. The model mesh was also required to resolve and separate the inlet and harbours main sub-tidal channels from the intertidal areas so that flooding and drying was well represented within the model. This becomes particularly important when considering the resuspension and transport of intertidal bed sediments.

Therefore, the initial step in setting up the model of Pahurehure Inlet and Southeastern Manukau Harbour in the region was to identify the main freshwater and sediment sources into the model domain. These outlets were identified following consultation with the ARC and are shown in Figure 1 and tabulated in Table 1.

Figure 1:
Catchment outlet locations used in the Southeastern Manukau Harbour and Pahurehure Inlet contaminant study.
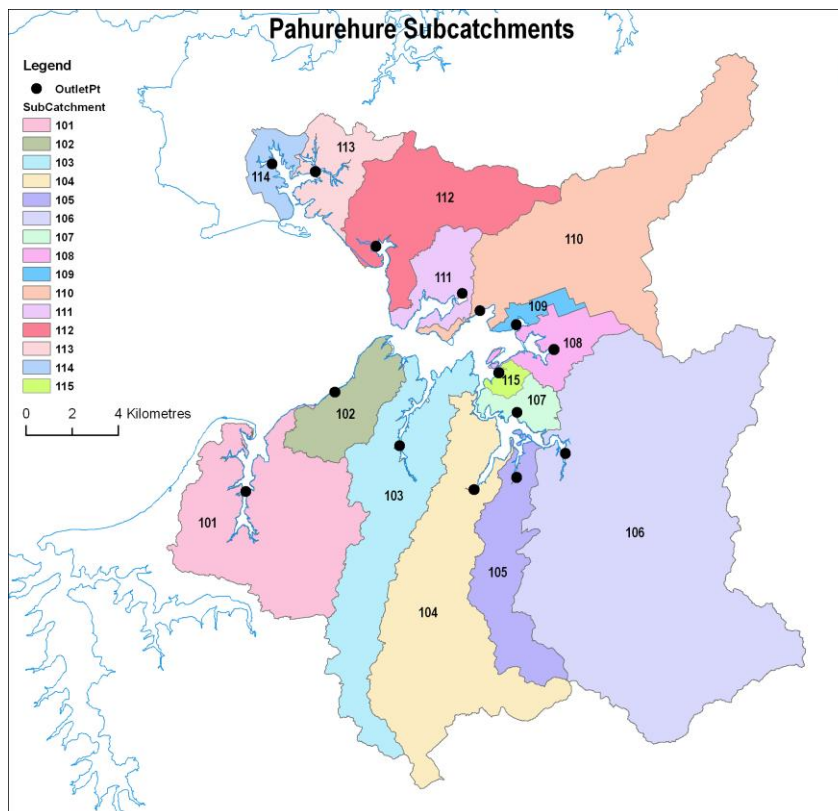
Table 1:

Numbers, names and codes of catchment outlets identified for inclusion as sources in to the MIKE3 FM model.

Code	Subcatchment
101 - KST	Kingseat
102 - EBH	Elletts Beach
103 - KKA	Karaka
104 - WHC	Whangapouri Creek
105 - OIC	Oira Creek
106 - DRY	Drury
107 - HGA	Hingaia
108 - PKA	Papakura
109 - TKI	Takanini
110 - PAS	Papakura Stream
111 - MAW	Manurewa / Weymouth
112 - PAU	Papatoetoe / Puhinui
113 - MEP	Mangere East / Papatoetoe
114 - MGE	Mangere
115 - BTB	Bottle Top Bay

3.1   Model Mesh Development

The model MIKE3 FM mesh was developed after consultation with the ARC who, in consultation with NIWA, defined and agreed the geographical regions of interest, the boundary limits and the freshwater/sediment source input sites.

The foundation of the present model grid was the greater Manukau Harbour model mesh (Bell et al.1998). This model was previously used in a study of 2-dimensional circulation in the greater Manukau Harbour. The Bell et al. (1998) model domain is shown in Figure 2. The bathymetric data extracted from the grid was then combined with high resolution Light Detection and Ranging imagery (LIDAR) data.

LIDAR is an aircraft-based remote sensing instrument used to collect highly accurate ground levels (relative to local chart datum). The regional coverage of the LIDAR image tiles are shown in Figure 3. Each of the Manukau Harbour and Pahurehure Inlet LIDAR image tiles consisted of approximately 1 point per 2 m^2 with height accuracy mostly 0.25 m. These data were processed into a series of mosaic images that were then further post-processed into bathymetric data that was incorporated into the model mesh. The processing of the raw LIDAR data to Chart Datum and into a format readable by the MIKE3 FM models was carried out as outlined in Appendix 1. This data was especially useful for increasing the resolution of the tidal creeks and mudflats. However, the channelised region of the estuary that remained flooded at times of low water was not penetrable by the LIDAR instrumentation. Therefore, as no additional bathymetric survey work was conducted by NIWA for the project, the bathymetry in the inner the upper regions creeks and tidal channels in the inlet were left to be resolved from archive aerial photography. This did leave some uncertainty on the shape, cross-section and depth of some of the creeks and channels. The impact of this is discussed in context of results and model calibration in later sections of this report.
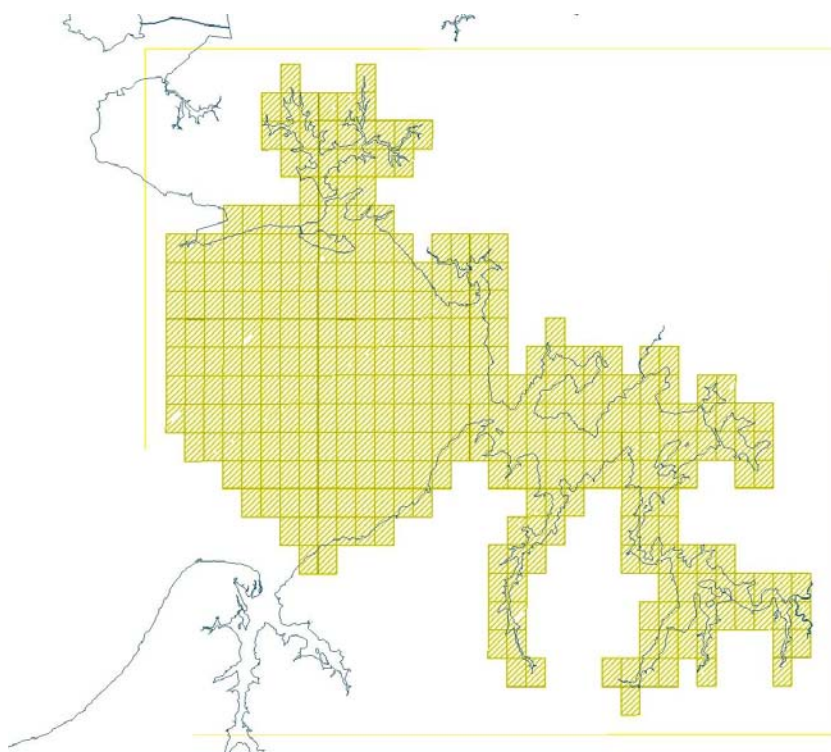
Figure 2:
Bathymetry data from the Manukau Harbour Model (Bell et al. 1998).
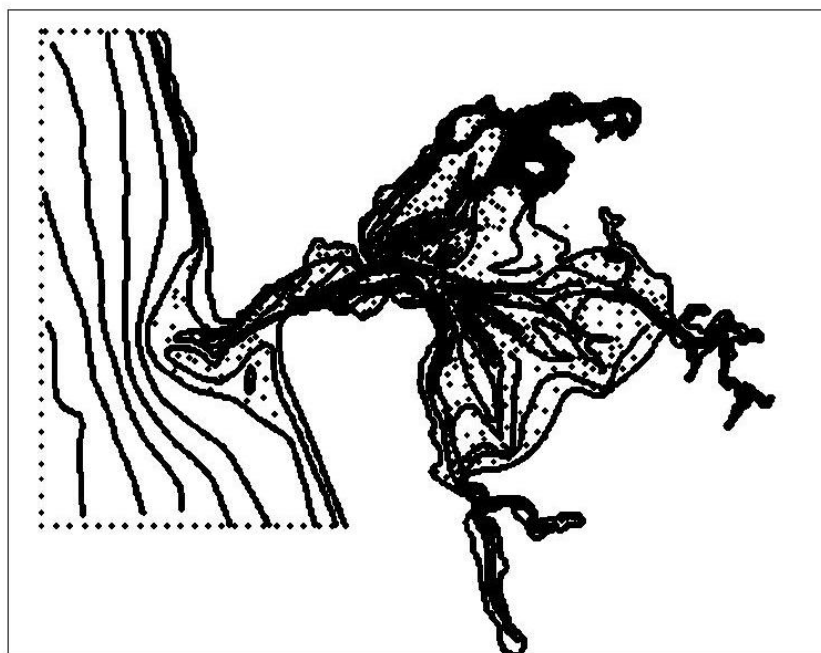
Figure 3:
LIDAR mosaics interpolated onto the Bell et al. (1998) harbour grid.

The finite mesh was then developed from the combined bathymetry data (Figure 2 and 4) by firstly interpolating the shoreline data every 150 m around the perimeter of the inlet and Southeastern Harbour region. The outer open ocean boundary and coast grid nodes were more widely spaced as to enlarge the element size and thus reduce resolution where no detail on sediment transport or deposition was required. Gridding was then carried out using a default minimum element angle of 28°, which resulted in the production of the mesh shown in Figure 4.

The subestuary boundaries for application of the USC model were defined on expert decision determined by the position of the catchment outlet, the channel bathymetry, and the wetting and drying effects on the hydrodynamics and sediment transport in the inlet. These are shown in Figure 5. The number of elements and areas for each of the subestuaries are shown in Table 2.

Table 2:

Subestuary element information. Code = Sub-estuary code number and name abbreviation; Subestuary = Subestuary name; No of Elements = Number of model mesh elements in the subestuary; Area = Sum of all element surface areas contained in subestuary; Sink = Subestuary defined as a sediment sink only in the USC3 model; Tidal Creek = Subestuary where a sediment from a source may be attenuated; Deep Channel = Subestuary where sediment may remain in suspension once it has been flushed from a source.

Code	Subestuary	No of Elements	Area (m²)	Sink	Tidal Creek	Deep Channel
1 -HIB	Hikihiki Bank	227	23840949			
2 - KKA	Karaka	23	385175			
3 - GMW	Glassons Mouth West	25	167768			
4 - GME	Glassons Mouth East	28	635090			
5 - CHN	Cape Horn	9	254352			
6 - DCO	Drury Creek Outer	43	1038072			
7 - PHI	Pahurehure Inner	88	1778269			
8 - PBA	Pahurehure Basin	14	172434			
9 - PKA	Papakura	58	1442876			
10 - KPT	Kauri Point	31	807656			
11 – WMC	Waimahia Creek	40	1193113			
12 - WEY	Weymouth	205	6014049			
13 - WIL	Wiroai Island	112	6511696			
14 - PUK	Puhinui Creek	34	562042		✓	
15 - PKK	Pukaki Creek	119	2246659		✓	
16 - DCI	Drury Creek Inner	423	3759221		✓	
17 - GCK	Glassons Creek Inner	195	982487		✓	
18 - CCK	Clarkes Creek	135	2379880		✓	
19 - MHW	Manukau Harbour	1643	727620739	✓		
20 - PCI	Pahurehure Channel Inner	65	1485889			✓
21 - PCO	Pahurehure Channel Inner	107	1920494			✓
22 - MNC	Manukau Channel North	288	10733603			✓
23 - MSC	Manukau Channel South	102	4749432			✓

Figure 4:

The MIKE3 FM mesh developed for this study. Note resolution of the mesh increases towards the east where the main attention of this study is focused. Bathymetry is shown with respect to local chart datum (Chart NZ4314).
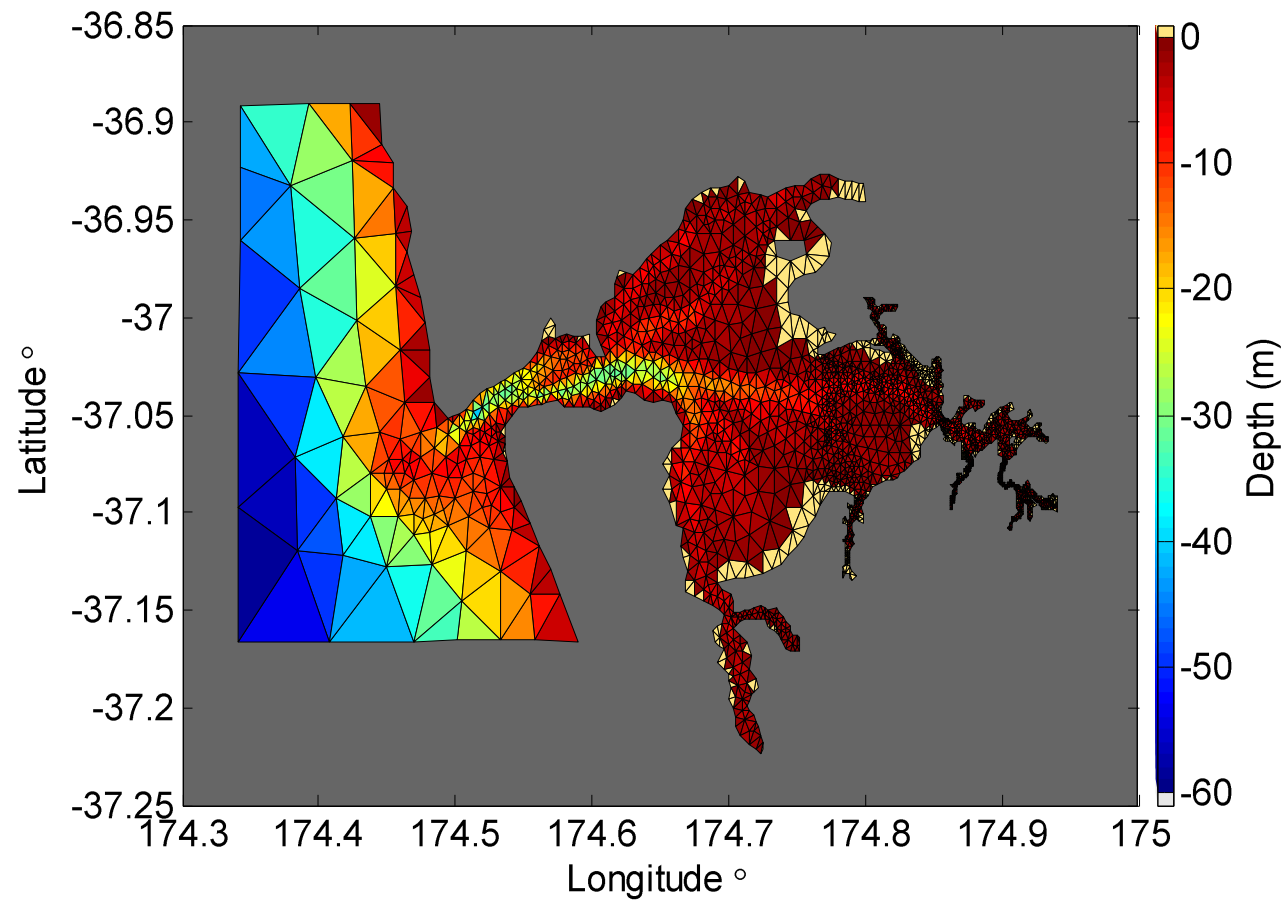
Figure 5:
Subestuaries defined from regional catchments and source outlets for application of the USC model. Subestuary size and classification are shown in Table 2.
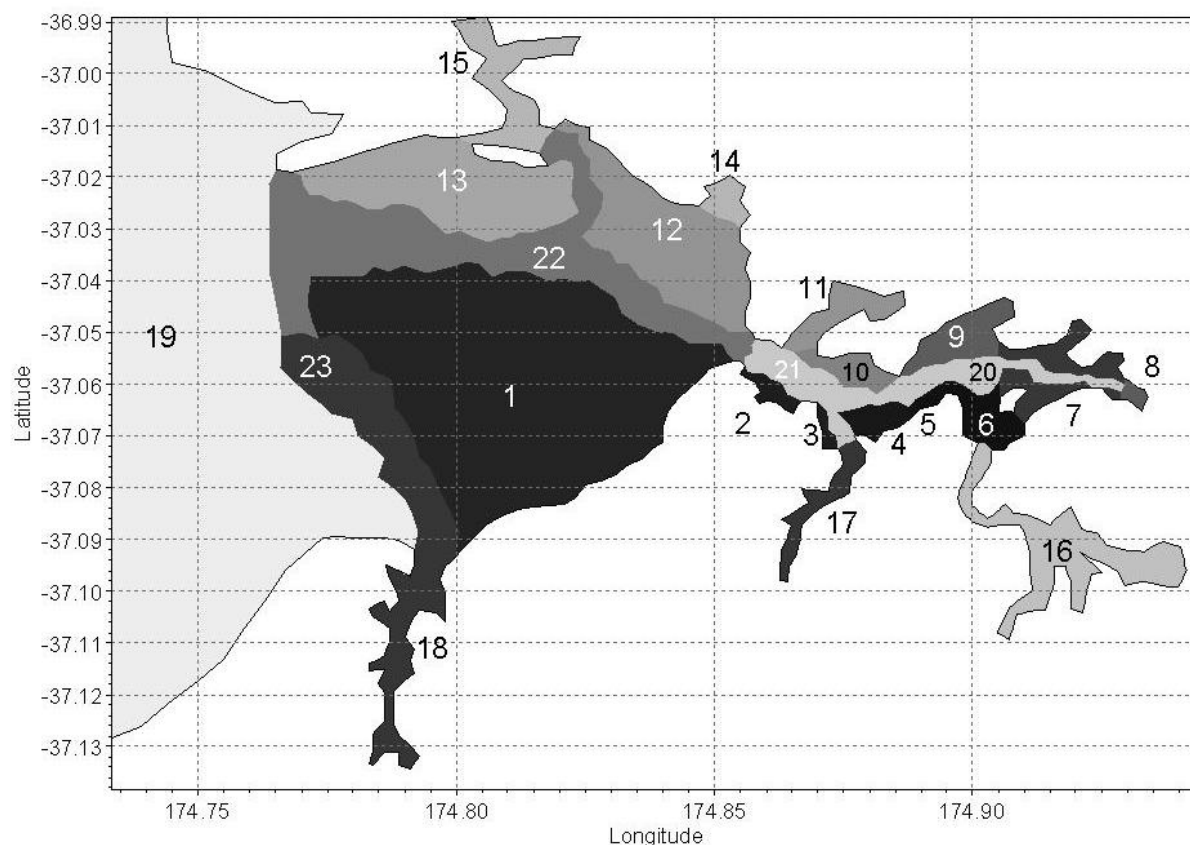
3.2 Fieldwork

A field program collected water levels, currents, salinities and suspended-sediment concentrations and wave statistics to calibrate and validate the MIKE3 FM and SWAN Models to observed field conditions. These data measured by current meters and DOBIE pressure tranduces (PT), optical backscatter scatter (OBS) and conductivity/temperature (salinity) sensors were deployed in the Pahurehure Inlet and Southeastern Manukau from 14 February 2007 and 26 March 2007 for deployment 1 (DP1) and 16 April 2007 and 29 May 2007 for deployment 2 (DP2). The positions of the instrumented study sites are shown in Figures 6a and 6b. A full description of the mooring and data collected are given in Pritchard et al. (2008).

Figure 6a:
DOBIE wave gauge sites used for calibrating the MIKE 3 FM and SWAN wave models. All DOBIEs measured water levels, optical backscatter and waves. DOBIEs at sites D3, D6, D7, D8 and D10 also measured conductivity and temperature. Sources indicate sites of freshwater and sediment input into the model. Grey area is land above MHWS. See Pritchard et al. (2008) for more specific details on instruments, instrument deployments, and mooring site locations.
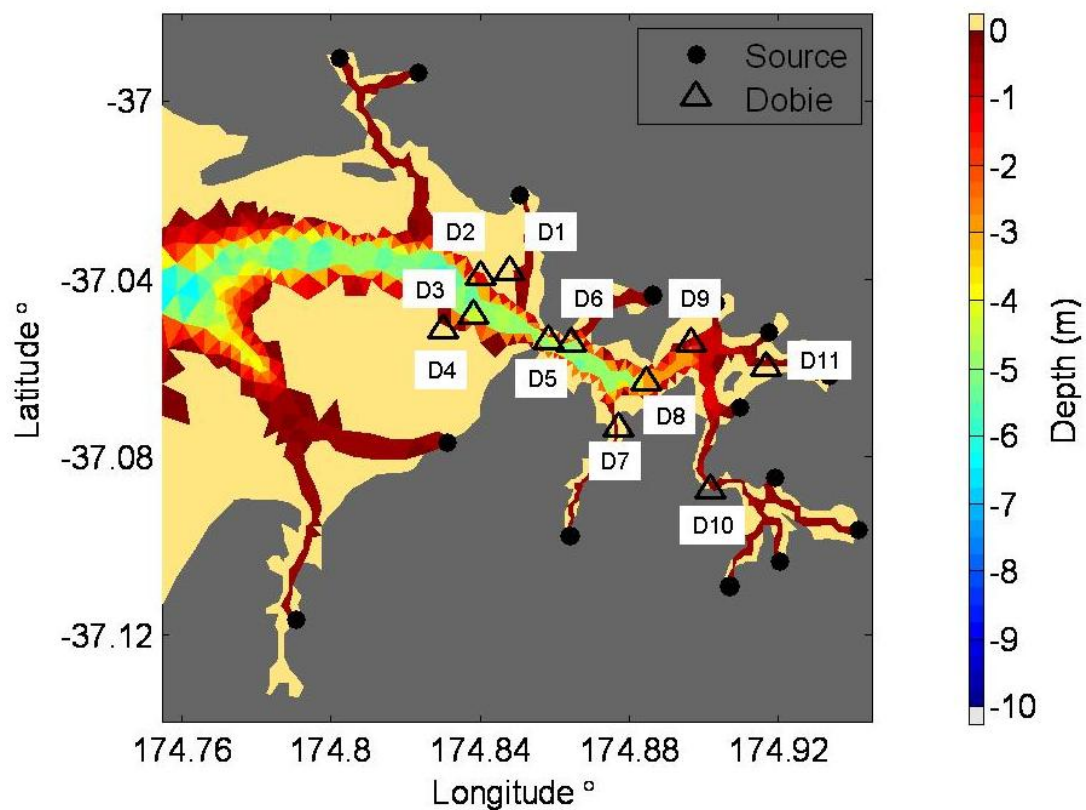
Figure 6b:

Current meter sites used for calibrating the MIKE3 FM and SWAN wave models. All DOBIEs measured water levels, optical backscatter and waves. Current meters at sites CM1, CM2, CM3, CM4 and CM5 also measured conductivity and temperature. Sources indicate sites of freshwater and sediment input into the model. Grey area is land above MHWS. See Pritchard et al. (2008) for more specific details on instruments, instrument deployments, and mooring site locations.
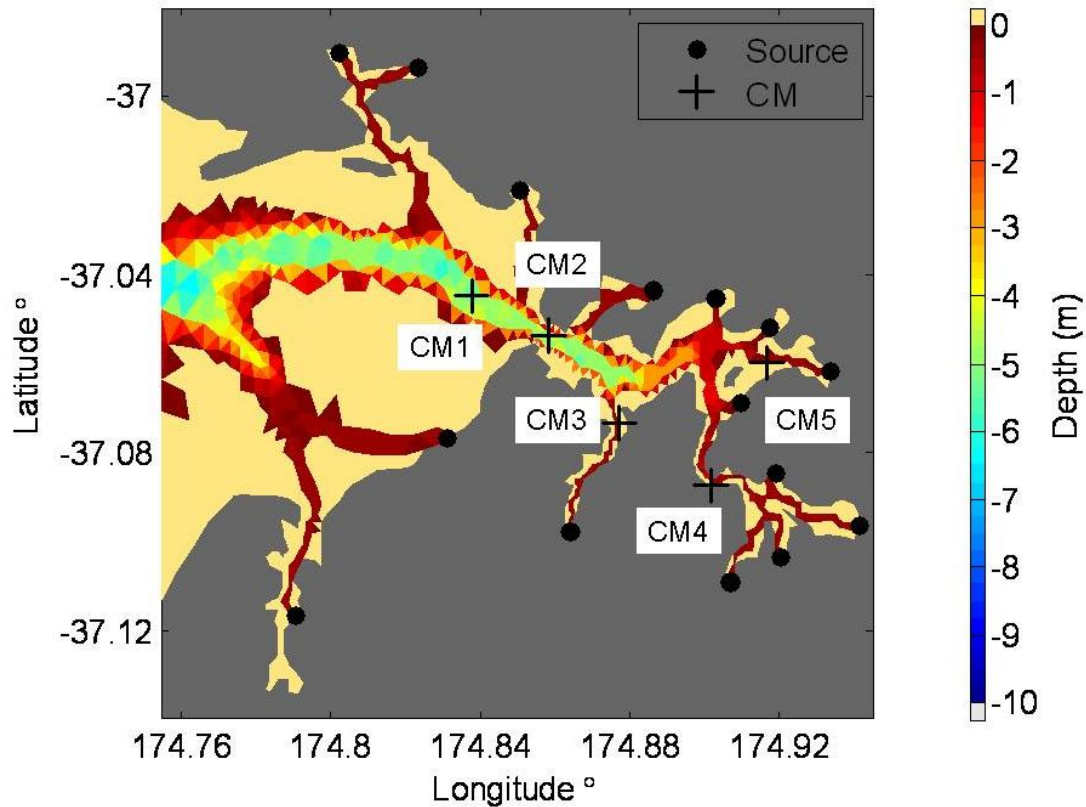
3.3   Summary

The Southeastern Manukau and Pahurehure Inlet model was developed on the basis of geographical boundaries, position of catchment discharge into the harbour and inlet.

The model mesh was then composed from archive data from an earlier modelling study of the region along with additional data from a recent ARC commissioned LIDAR survey of the Southeastern Manukau and Pahurehure Inlet. The resultant FM mesh was then compartmentalized in to sub-estuary regions to be later used in the USC model.

During February 2007 to late May 2007 two field deployments of instruments were used to collect data that would be later used to calibrate the MIKE3 FM model. .

4 Model setup and calibration

The setup and calibration of the MIKE3 FM HD and MT models consisted of comparing model output and the measured water levels, currents, salinities and suspended-sediment concentrations (SSC) to observed field conditions.

This required various model calibration parameters to be adjusted until the comparisons between observed and modelled values were satisfactory. A brief physical description and formulation of the processes that were calibrated are described in Appendix 2. A list of the specific model set up and simulation details are also shown in Table A2 of the appendix.

The SWAN model was similarly calibrated against measured wave heights and periods.

4.1 Offshore Tidal Boundary Conditions

Tidal forcing at the models offshore oceanic boundary was computed from EZZY-tide predictions. These are a series of geographically site specific (depending on bathymetry) dominant tidal constituent constants that are generated by a detailed NIWA tidal model of New Zealand coastal waters (Walters et al. 2001). These constants can be used to predict tidal elevation levels at the offshore boundary for any specific time period or duration. A list of the tidal constituents used to drive the offshore boundary condition is shown in Table A2.

4.2 Water surface elevation

The 2007 DOBIE (pressure sensors) mooring data were used to calibrate the barotropic tide elevation. These data were compared to the MIKE3 FM HD model simulations that predicted elevations for the time corresponding to the periods of instrument deployment where the model was forced using the EZZY tide offshore boundary condition.

Bed roughness z_0 was varied to achieve the best fit between measured and predicted water surface elevations. The roughness that gave the best fit is shown in Figure 7. Figure 8 shows the observed and modelled water surface elevations at sites D3, D5, D7, D10 and D11 for deployment period DP1 (14 February 2007 - 26 March 2007). These particular sites were selected because they also correspond to where current meters were deployed as shown in Figure 6b.

The modelled elevations were compared to the observed through a cross-correlation (cross-covariance analysis) between the two time series. This gave a measure of similarity of between the two signals (Emery and Thompson, 2001). The results from the simulations showed good agreement with the observed tidal phase having a >0.95 cross-correlation coefficient for all five sites. Nevertheless, there was evidence of discrepancy in the absolute high water/low water amplitude at three of the inner inlet and creek sites. Model predictions in the creeks tended to under estimate elevations

at times of observed low water i.e. Root mean square error (RMSE) of O (0.05 m). These discrepancies arise from differences in the actual and model bathymetry and minor tidal constituents (sub-harmonics) not included in the boundary forcing. This is further compounded by localised roughness and frictional effects. The limitations arising from these small water level differences are discussed in more detail in the Section 4.3.

Figure 7:
Bed roughness (z0) used in MIKE3 FM HD model setup.
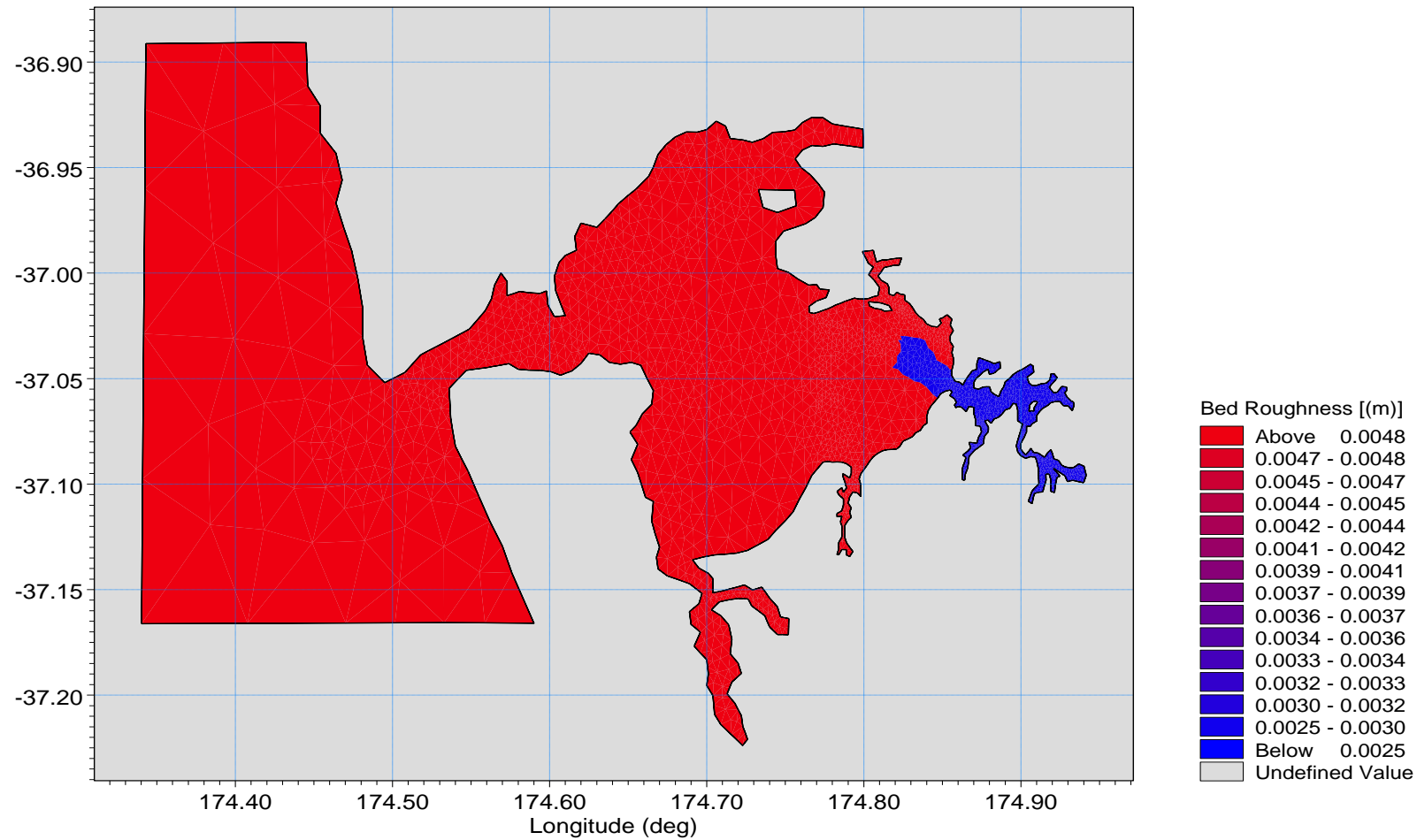
Figure 8:

Observed and modelled water surface elevation at sites D3, D5, D7, D10 and D11 for DP1. RMSE errors were O(0.05 m).

Southeastern Manukau Harbour/Pahurehure Inlet Contaminant Study:
Hydrodynamic wave and sediment transport model implementation and calibration

24

4.3　Currents

Having calibrated for water levels, the same five sites were selected to calibrate the model currents (see Figure 6b).

Figures 9a-9e show comparisons between the observed and modelled current vectors: u (East-West); v (North-South) for the first and most complete series of current meter deployments (DP1). All current meter records extended to over 30 days of data and as consequence could be analysed for the duration of one complete spring-neap cycle.

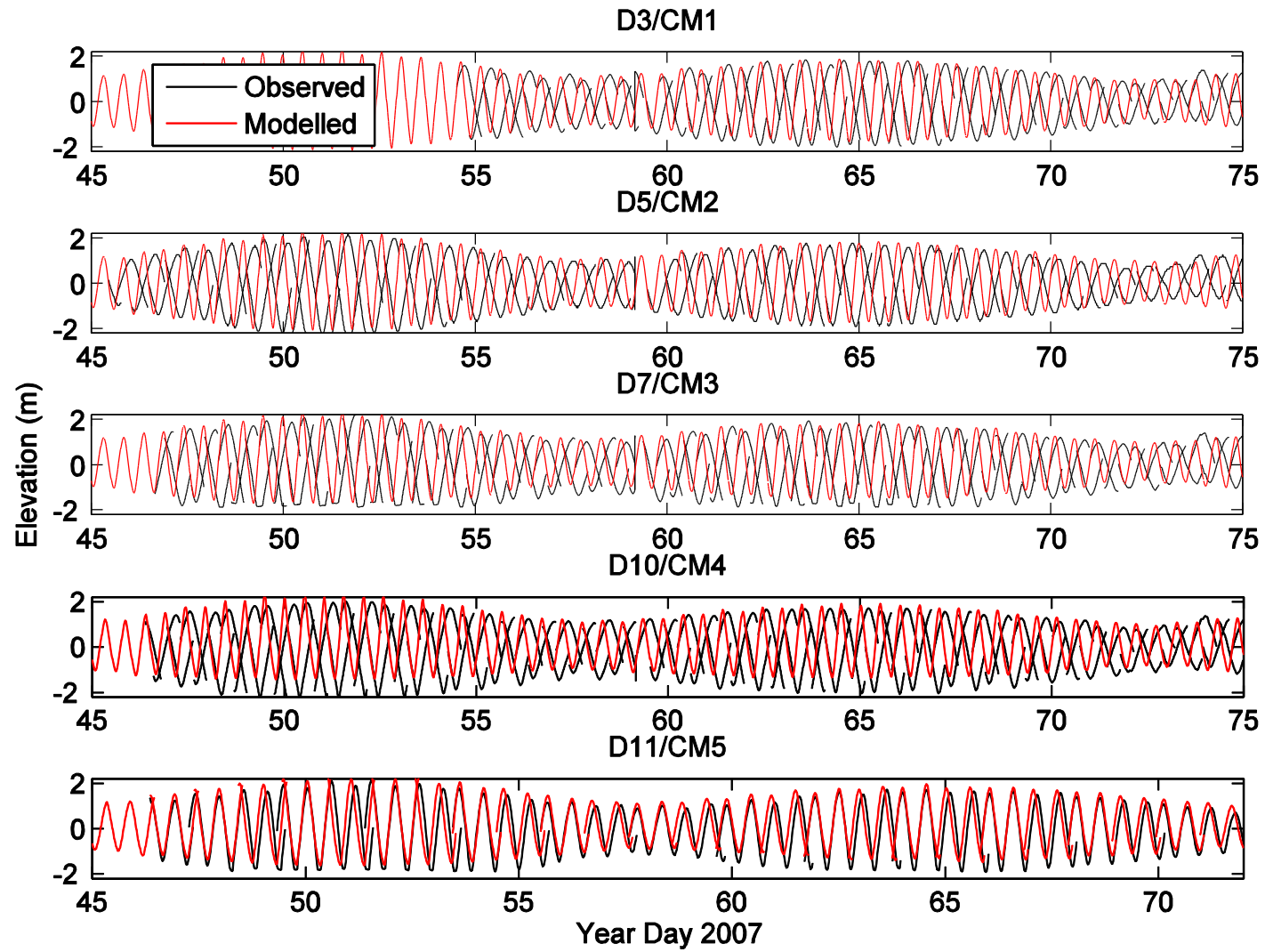The best overall fit between observed and modelled currents was obtained by using a Smagorinsky coefficient of 0.42 for the horizontal eddy viscosity formulation, with a lower bound of 1.8e-006 m^2 s^{-1} and an upper bound of 10 m^2 s^{-1}.

For the vertical eddy viscosity, the constants c_1 and c_2 were set to 0.41 and -0.41, respectively, to give a standard parabolic profile. The upper and lower limits of the vertical eddy viscosity were set to 1.8e-006 m^2 s^{-1} and 0.4 m^2 s^{-1}, respectively, which are the default values used in the MIKE3 FM HD model. Model tests showed very little difference in predicted currents at any of the sites with adjustments to the vertical eddy viscosity. The value for the wind-induced surface shear stress drag coefficient (c_d) was set to the default value of 0.00125. Adjustment (± 0.0005) showed no significant improvements to model predictions.

Modelled and observed currents showed generally good (by eye) agreement at most of the measured sites. However, in some of the narrow channels and creeks there were some clear discrepancies between the observed and predicted currents.

For example, at sites CM3 and CM4 shown in Figure 9c and 9d where there was an obvious disparity in the direction of observed and predicted currents. The effect of this discrepancy can be best shown through a comparison of the observed and modelled currents using a progressive vector diagrams. Figure 10a and 10b are plots of the time integrated current vectors. Both illustrate a net outward direction of flow from the two creeks for both predicted and observed values consistent with a 'source input'. However, although current magnitudes are in reasonable agreement, direction of the flows is slightly offset. Observed values show a more westerly directed flow. This shows the sensitivity of the observed flow to small localised changes in the shape of channel bathymetry that are not fully resolved in the model mesh. As noted in Section 4.2 some further minor discrepancies in the modelled currents could also arise from the incorrect or non resolution of localised harmonics generated by changes in the bathymetry and bottom friction.

Table 3a to 3e show the results from a least squares tidal harmonic analysis (Pawlowicz et al. 2002) of both modelled and observed current phase and amplitude for each of the five current meter sites. Current amplitude was defined in terms of the ellipse major amplitude (maximum tidal current along the principal axis of the current) and ellipse inclination (peak tidal current direction relative to True North), and ellipse phase (time of the peak tidal current relative to NZST). Only tidal constituents with signal to noise ratios (SNR) >10 are reported.

The analysis shows that the majority of the explained tidal variance in current meter measurements and model predictions is accounted for by the semi-diurnal tides. The principle lunar (M_2) provided the major astronomical forcing of currents at each respective site. The other semi-diurnal and longer period constituents explained lower levels of variance in the observed and modelled tidal currents

Overall, the observed and modelled phase, and inclination for the M_2 constituent are in generally good agreement. However, the observed and modelled M_2 current amplitudes show a mean difference of 34% over the five sites. This difference cannot be attributed to tidal energy dissipation between the offshore boundary and the harbour and inlet. The more likely cause is through localised bathymetric effects not accounted for in the model mesh.

Figure 9a:

Observed and modelled water currents at D3/CM1 (Papakura Channel).
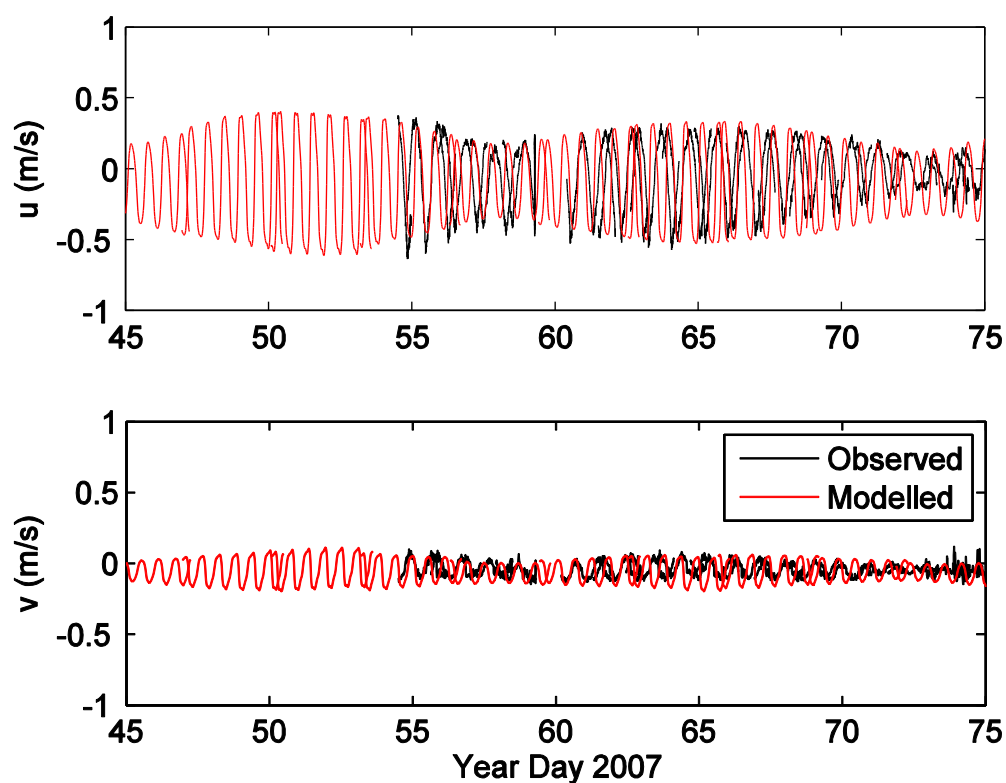
Table 3a:

Comparison of measured and predicted tidal current ellipses at Site D3/CM1 (Papakura Channel).

Location	Observed Amplitude (m s⁻¹)	Observed Inclination (° True)	Observed Phase (° NZST)	Modelled Amplitude (m s⁻¹)	Modelled Inclination (° True)	Modelled Phase (° NZST)	Difference Amplitude (m s⁻¹)	Difference Inclination (°)	Difference Phase (°)
P1 Larger Solar Declin	0.02	168	72	0.01	165	186	0.01	3	114
K1 Luni-Solar Declin	0.02	168	85	0.01	165	150	0.01	3	65
N2 Larger Lunar Elliptic	0.05	166	8	0.08	165	60	0.04	1	54
M2 Principle Lunar	0.26	168	56	0.40	165	55	0.18	3	1
S2 Principle Solar	0.07	172	192	0.11	165	110	0.06	7	7
K2 Luni-Solar Declin	0.08	173	38	0.02	165	70	0.06	8	8

Southeastern Manukau Harbour/Pahurehure Inlet Contaminant Study:
Hydrodynamic wave and sediment transport model implementation and calibration

27

Figure 9b:

Observed and modelled water currents at D5/CM2 (Te Pua Point).
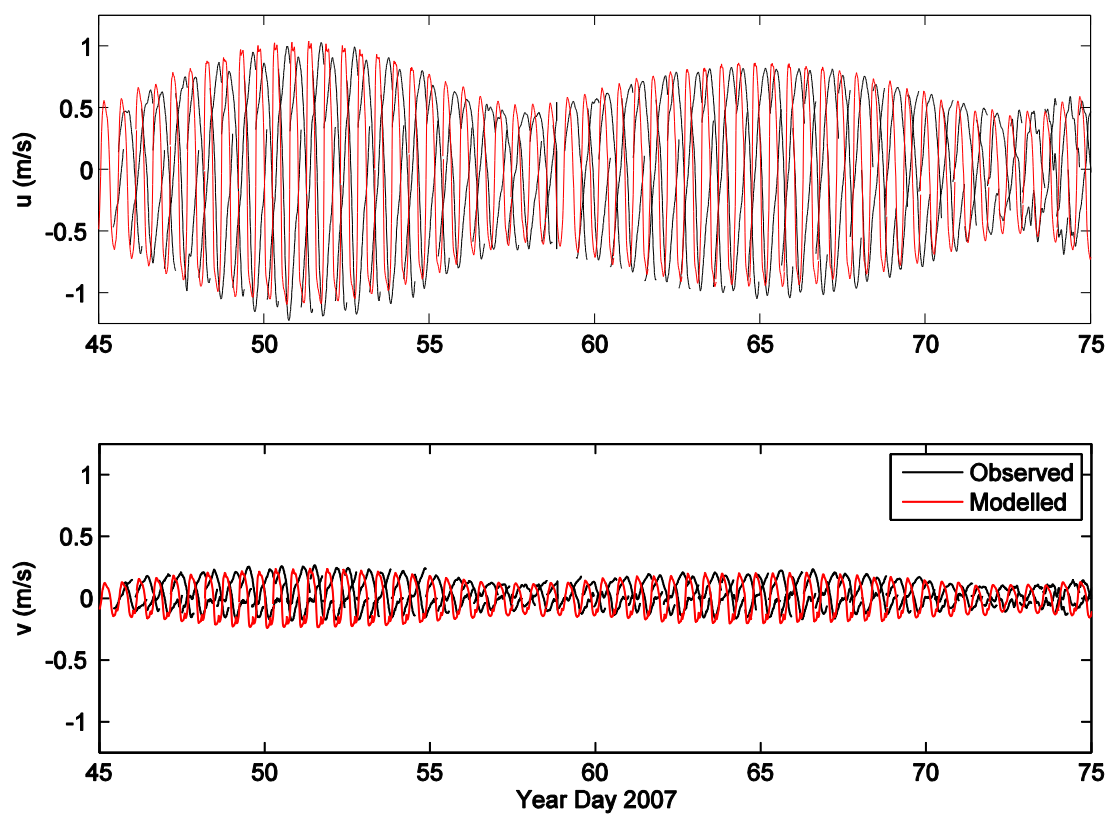
Table 3b:

Comparison of measured and predicted tidal current ellipses at Site D5/CM2 (Te Pua Point).

Location	Observed			Modelled			Difference		
	Amplitude (m s⁻¹)	Inclination (° True)	Phase (° NZST)	Amplitude (m s⁻¹)	Inclination (° True)	Phase (° NZST)	Amplitude (m s⁻¹)	Inclination (°)	Phase (°)
P1 Larger Solar Declin	0.01	11	305	0.01	12	8	0.00	1	117
K1 Luni-Solar Declin	0.03	9	302	0.03	12	331	0.00	3	29
N2 Larger Lunar Elliptic	0.14	8	231	0.17	11	240	0.03	3	9
M2 Principle Lunar	0.70	9	230	0.88	11	236	0.18	2	6
S2 Principle Solar	0.19	9	270	0.25	11	291	0.06	2	21

Southeastern Manukau Harbour/Pahurehure Inlet Contaminant Study:
Hydrodynamic wave and sediment transport model implementation and calibration

28

Figure 9c:
Observed and modelled water currents at D7/CM3 (Glassons Creek).
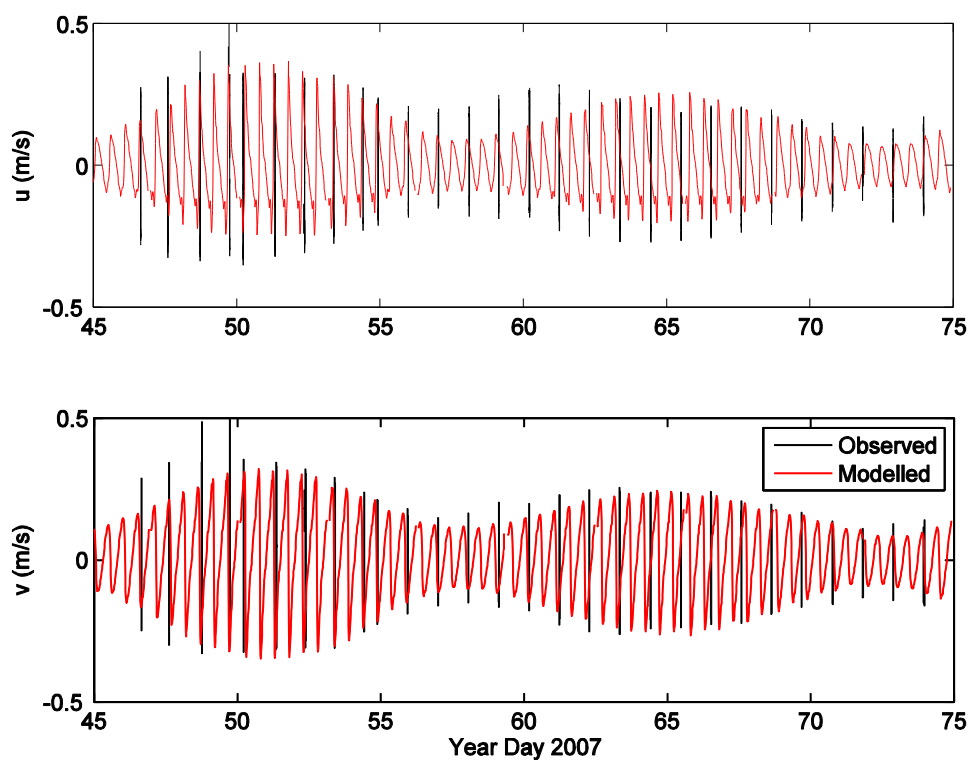
Table 3c:

Comparison of measured and predicted tidal current ellipses at Site D7/CM3 (Glassons Creek).

Location	Observed Amplitude (m s^{-1})	Observed Inclination (° True)	Observed Phase (° NZST)	Modelled Amplitude (m s^{-1})	Modelled Inclination (° True)	Modelled Phase (° NZST)	Difference Amplitude (m s^{-1})	Difference Inclination (°)	Difference Phase (°)
P1 Larger Solar Declin	0.04	141	312	0.00	142	194	0.04	1	118
K1 Luni-Solar Declin	0.03	107	342	0.01	145	154	0.02	38	8
N2 Larger Lunar Elliptic	0.07	140	65	0.03	142	63	0.05	2	2
M2 Principle Lunar	0.29	137	58	0.16	142	54	0.13	5	2

Southeastern Manukau Harbour/Pahurehure Inlet Contaminant Study:
Hydrodynamic wave and sediment transport model implementation and calibration

29

Figure 9d:

Observed and modelled water currents at D10/CM4 (Drury Creek).
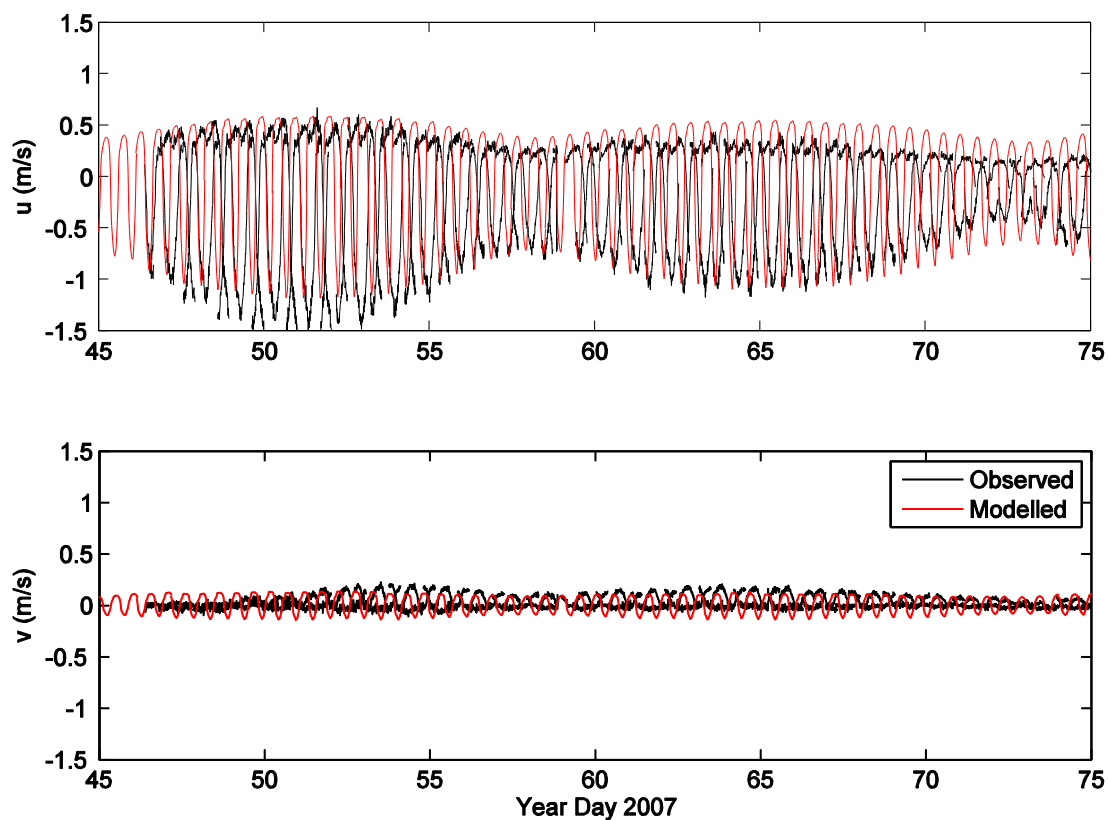
Table 3d:

Comparison of measured and predicted tidal current ellipses at Site D10/CM4 (Drury Creek).

Location	Observed			Modelled			Difference		
	Amplitude (m s^{-1})	Inclination (^{o} True)	Phase (^{o} NZST)	Amplitude (m s^{-1})	Inclination (^{o} True)	Phase (^{o} NZST)	Amplitude (m s^{-1})	Inclination (^{o})	Phase (^{o})
P1 Larger Solar Declin	0.02	2	261	0.01	178	28	0.01	176	53
K1 Luni-Solar Declin	0.02	178	91	0.02	179	352	0	1	6
M2 Principle Lunar	0.59	173	74	0.72	171	69	0.13	2	5
S2 Principle Solar	0.17	1	328	0.19	171	156	0.02	170	8

Southeastern Manukau Harbour/Pahurehure Inlet Contaminant Study:
Hydrodynamic wave and sediment transport model implementation and calibration

30

Figure 9e:

Observed and modelled water currents at D11/CM5 (Pahurehure Inlet Channel).
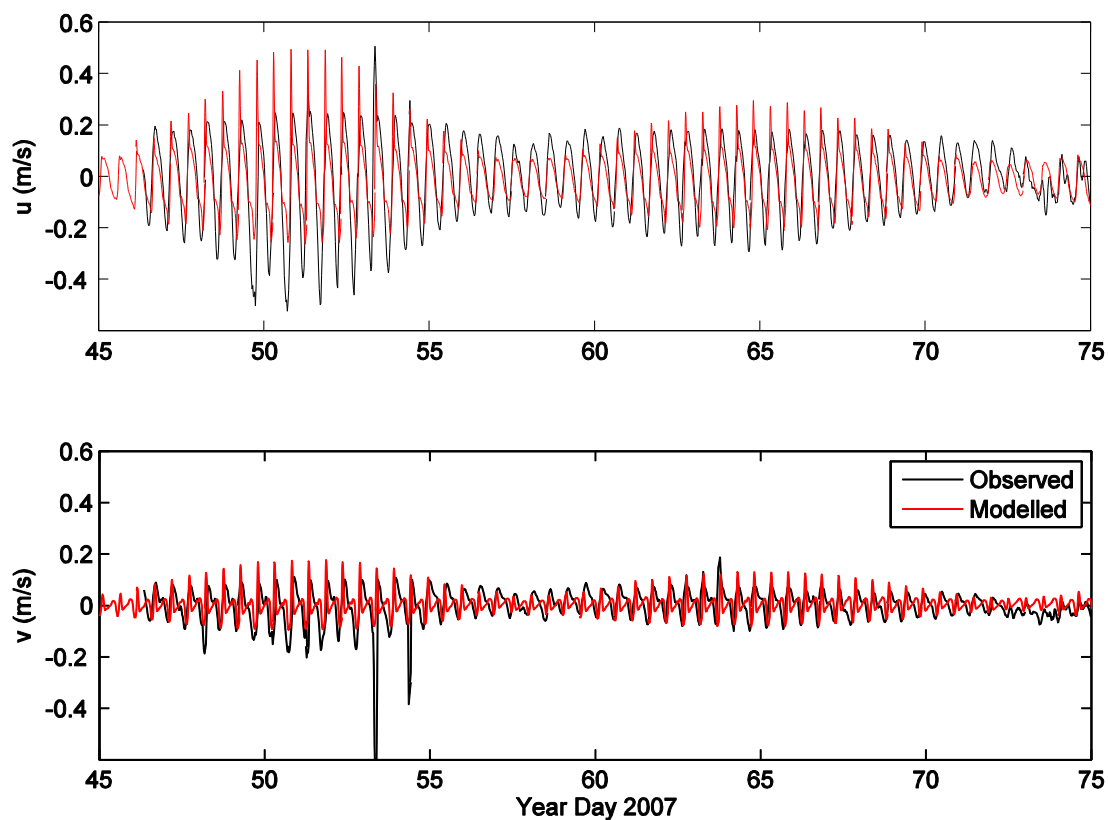
Table 3e:

Comparison of measured and predicted tidal current ellipses at Site D11/CM5 (Pahurehure Inlet Channel).

Location	Observed			Modelled			Difference		
	Amplitude	Inclination	Phase	Amplitude	Inclination	Phase	Amplitude	Inclination	Phase
	(m s^{-1})	(^{o} True)	(^{o} NZST)	(m s^{-1})	(^{o} True)	(^{o} NZST)	(m s^{-1})	(^{o})	(^{o})
K1 Luni-Solar Declin	0.03	180	116	0.00	9	326	0.03	171	210
N2 Larger Lunar Elliptic	0.05	18	235	0.03	6	237	0.02	12	2
M2 Principle Lunar	0.19	17	239	0.12	4	234	0.07	13	5
S2 Principle Solar	0.06	159	123	0.04	123	281	0.02	36	158
M4 – Quarter SD	0.06	30	344	0.06	36	28	0.00	6	40

Figure 10a:

Southeastern Manukau Harbour/Pahurehure Inlet Contaminant Study:
Hydrodynamic wave and sediment transport model implementation and calibration

31

Progressive vector diagram showing the observed and modelled data at site CM3 (Glassons Creek).
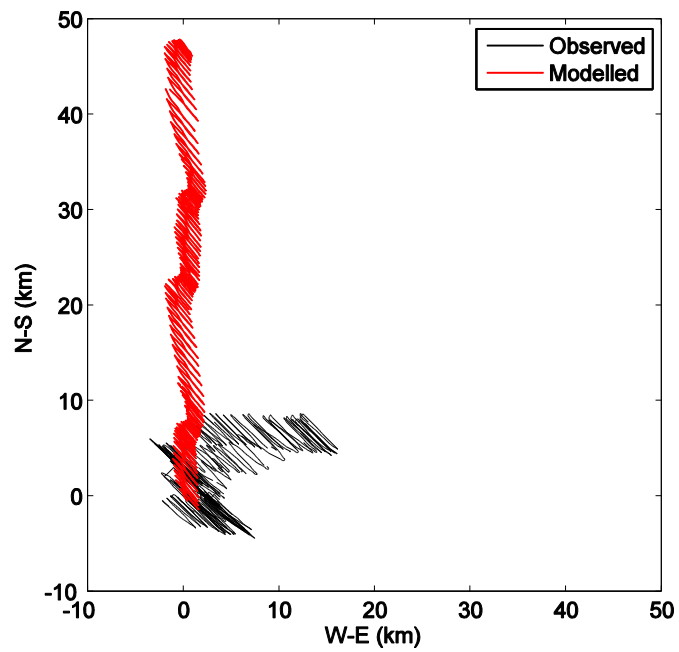
Figure 10b:

Progressive vector diagram showing the observed and modelled data at site CM4 (Drury Creek).
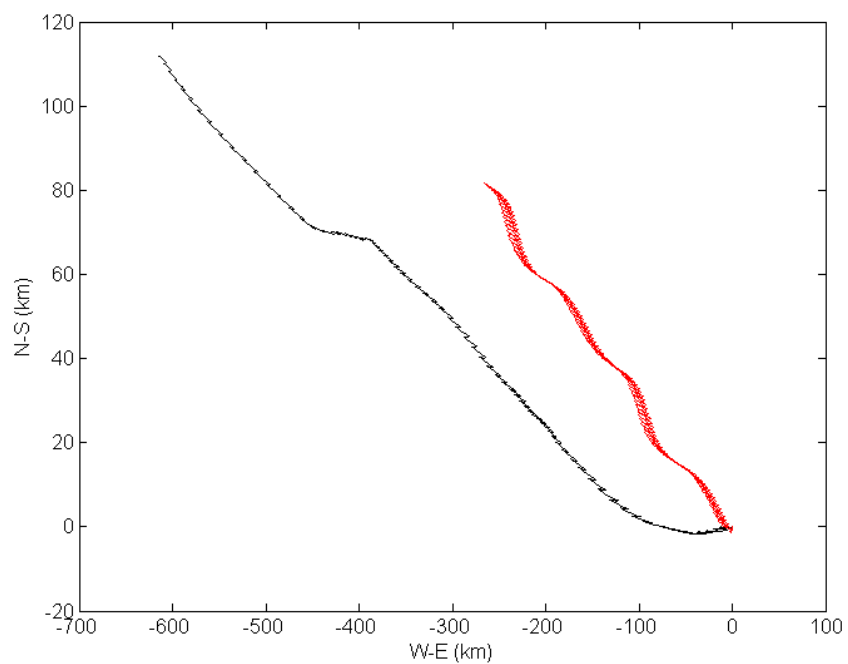
4.4   Salinity

The model capability to simulate the horizontal and vertical salinity distributions in the harbour and tidal creeks was evaluated for both deployment 1 (DP1) between 15 February-26 March 2007 and deployment 2 (DP2) 24 April -29May 2007.

Figure 11a:
Wind speed and direction and daily rainfall as recorded at Auckland Airport during the 2007 DP1 deployment period (14/2/07 - 26/3/07).
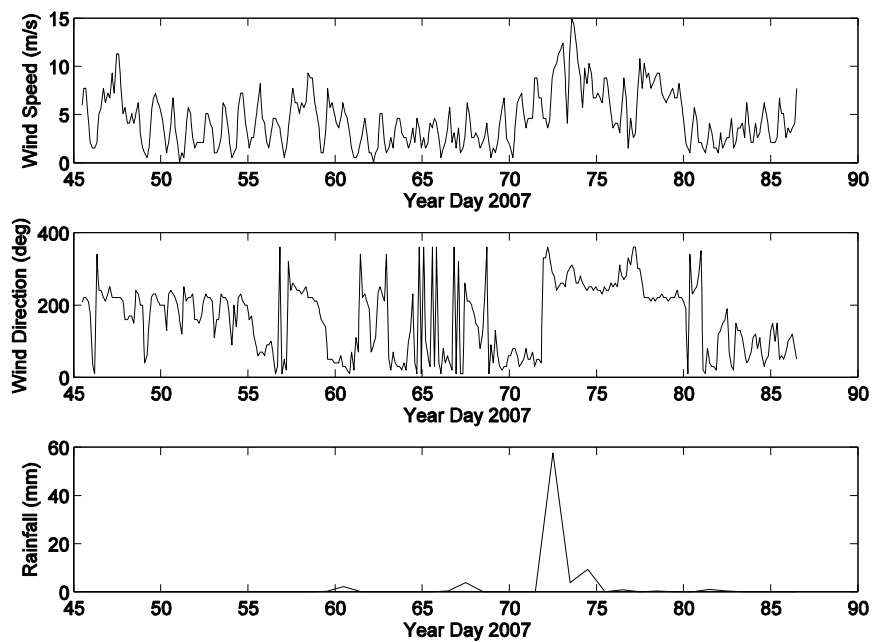
Figure 11b:
Wind speed and direction and daily rainfall as recorded at Auckland Airport during the 2007 DP2 deployment period ((16/4/07-29/5/07).

Figure 11a and Figure 11b show the corresponding daily averaged time series of rainfall, wind speed and direction recorded at Auckland Airport during both of the 2007 field programs.

Figure 11a shows that during DP1 only one major rainfall event was recorded when nearly 60 mm fell during a 24 hour period. Similar dry conditions were also recorded during DP2 as shown Figure 11b when only around 20 mm fell in early May with the rest of the deployment period remaining practically dry.
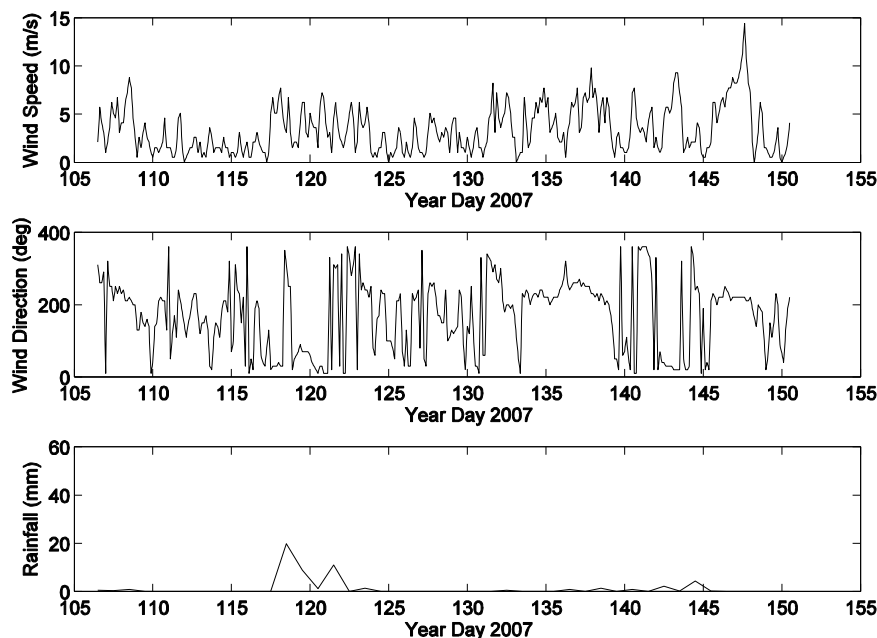
The lack of any extended periods of precipitation through both mooring deployments limited the model salinity calibration for the majority of the observational study to baseline (low) freshwater source inflow rates. These inflow rates were provided by the NIWA water resources data base. The additional increase in discharge caused by the few days of rain recorded during the two calibration periods was then converted to outflow rates based on the TP108 approach (ARC, 1999). These values were then combined with the baseline flow rate for the model salinity calibration.

The model was initially spun up for 14 days with an offshore ocean boundary salinity set at 34.5 PSU. This value was also used as the initial value through the whole model domain. During spin-up (model ran until stable), freshwater inflow rates were set at baseline levels at all sources. Then at the end of the spin-up period, freshwater inflows derived from TP108, and predicted tides and measured winds, were used to model the salinity in the harbour during the DP1 and DP2 deployment periods.

Figure 12a and Figure 12b show the resultant modelled and observed salinity during DP1 and DP2 deployment periods. The predicted salinity values are interpolated to the approximate depth of the respective temperature-conductivity (CT) sensor for each of the five instrumented sites where time series data were collected.

Southeastern Manukau Harbour/Pahurehure Inlet Contaminant Study:
Hydrodynamic wave and sediment transport model implementation and calibration

34

Figure 12a:

Observed and Modelled salinity measured between 15 February-26 March 2007 during deployment 1 (DP1) of the field program at 5 sites for in the Southeastern Manukau Harbour and Pahurehure Inlet. See Figure 1a for specific mooring locations.

Southeastern Manukau Harbour/Pahurehure Inlet Contaminant Study:
Hydrodynamic wave and sediment transport model implementation and calibration

35
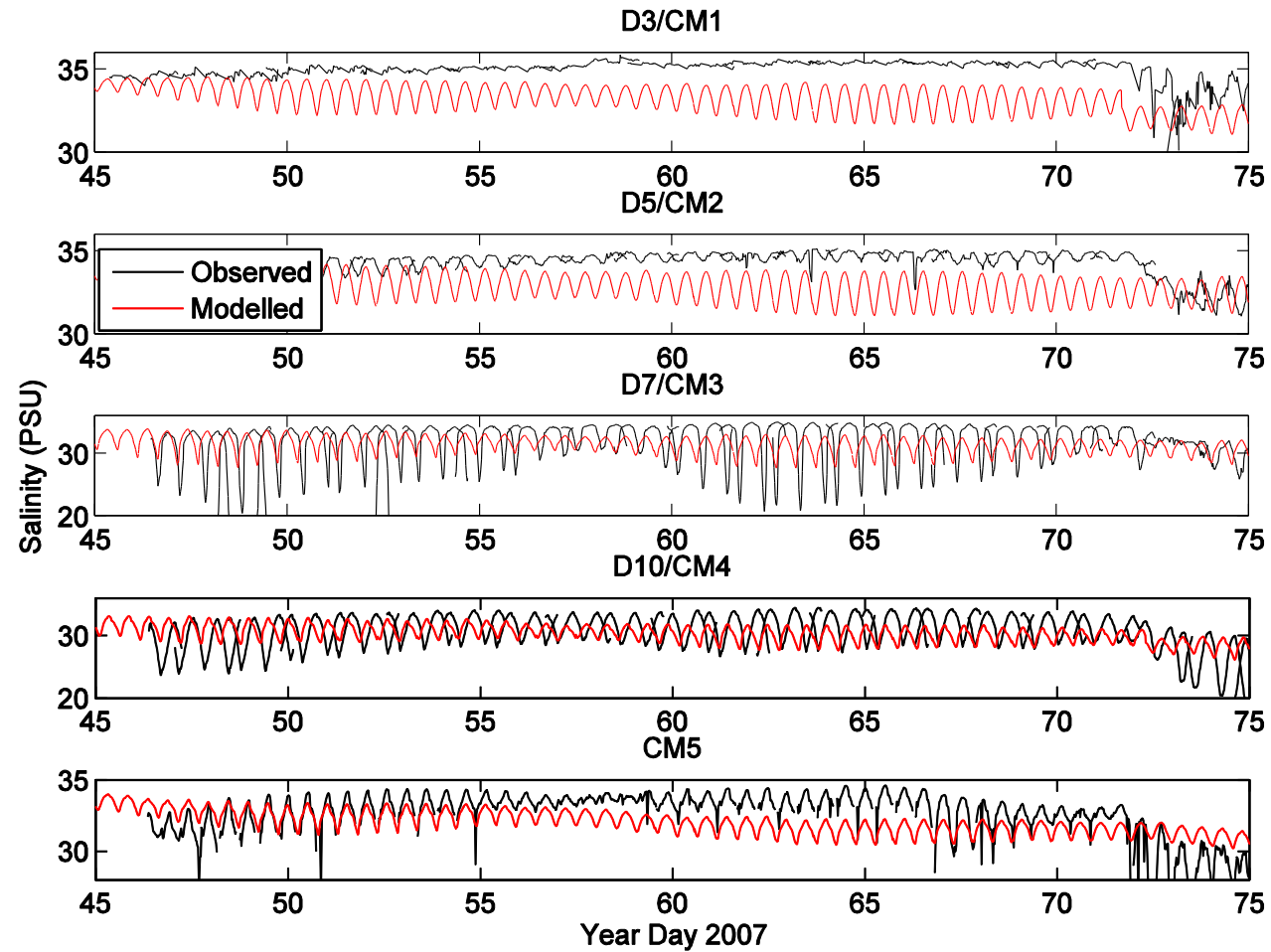
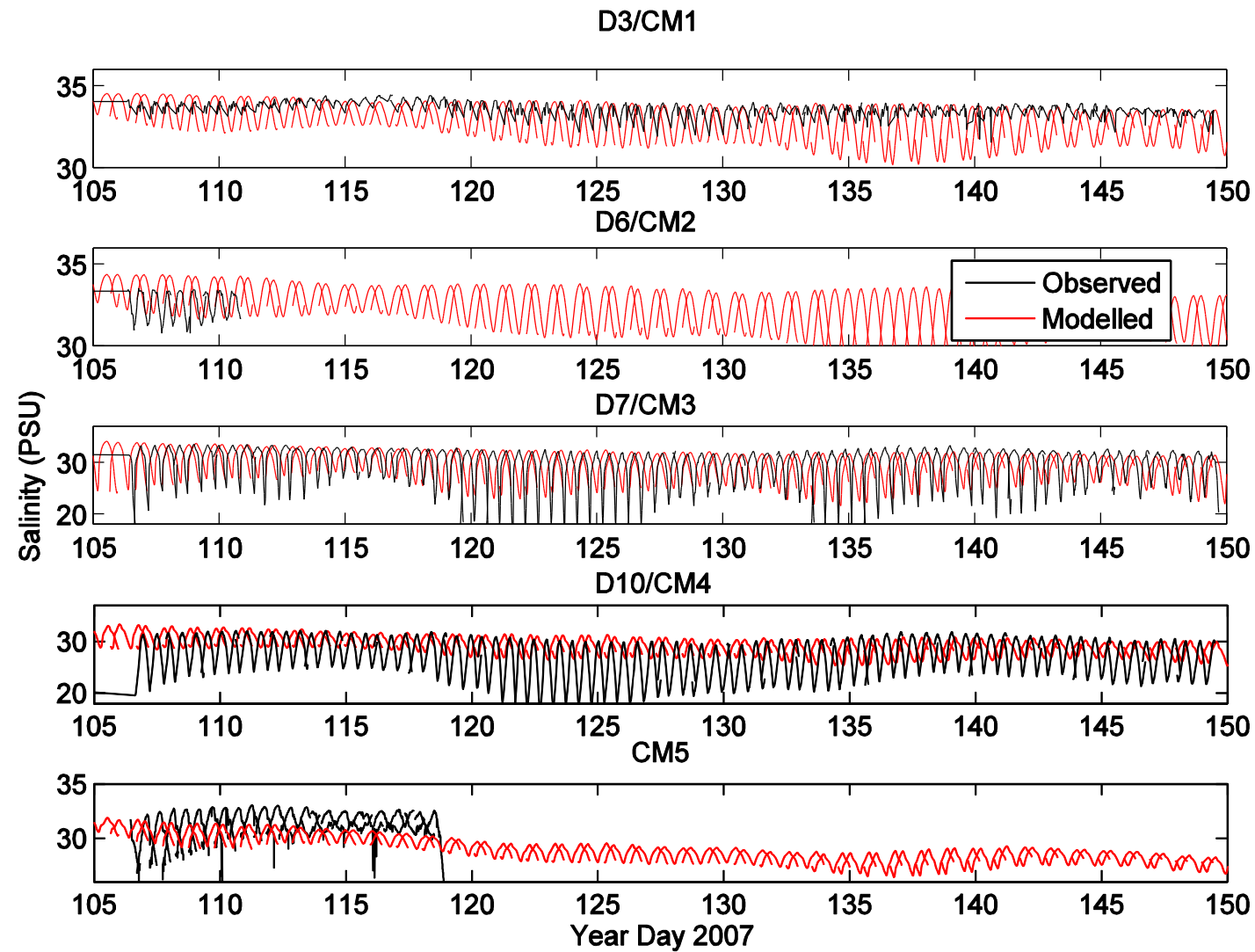**Figure 12b:**

Observed and Modelled salinity measured between 24 April -29 May 2007 during deployment 2 (DP2) of the field program at 5 sites for in the Southeastern Manukau Harbour and Pahurehure Inlet. See Figure 1a for specific mooring locations.

Southeastern Manukau Harbour/Pahurehure Inlet Contaminant Study:
Hydrodynamic wave and sediment transport model implementation and calibration

36

The comparisons between the observed and modelled salinity shows that for most of the instrumented sites, through the duration of both deployments, the phase change in salinity through tidal advection was well simulated. This was especially evident in the two tidal creeks, D7 (Glassons Creek) and D10 (Drury Creek) where the majority of fresh water was discharged into the Pahurehure Inlet. The differences in the amplitude of the observed and modelled salinity changes was a limitation of predicting source discharge magnitude from the estimates of baseline flow and the assumptions of the TP108 approach. Underestimation of the salinity change brought about by tidal advection in the creeks indicated the predicted freshwater source inflow rates were slightly low. By artificially increasing the rates, there was some improvement. However, it was decided to remain consistent with the database values so as to prevent any conflict with other parts of the study methodology used in later application of the model to the USC modelling.

The measurements recorded at the three instrumented sites situated out in the inlet and inner harbour (D3, D6, CM5) tended to show the greatest discrepancy with the modelled values. During DP1, the observed salinities at sites D3 and CM5 showed little deviation from ambient ocean water values. However, during DP2 there was better agreement between observed and modelled values at site D3. At site CM5 comparisons with the model predictions at the start of DP2 showed promise until the instrument failed.

Both the vertical and horizontal dispersion coefficients for salinity were applied through a scaling factor that relates vertical and horizontal mixing to the eddy viscosity formulation. The best overall fit between observed and predicted salinity was obtained by applying a scale factor of 1.1 in both the horizontal and vertical dimensions. Lower dispersion values tended to under-estimate vertical mixing and hence damping the salinity oscillations. Higher values led to rapid mixing in the horizontal, which removed the small oscillations in salinity measurements observed especially during DP2 outside the tidal creeks.

This calibration procedure also highlighted the sensitivity of the model eddy viscosity parameterization of turbulence to bathymetric (depth) and channel shape variation. Furthermore, this problem could be compounded by applying a 'broad brush' turbulence value to both channelized and open water sites. Hence, a general compromise for the whole domain had to be reached through using a scaling factor = 1.1.

4.5 SWAN model application to the Southeastern Manukau Harbour and Pahurehure Inlet

A SWAN wave model domain was established covering the Southeastern Manukau Harbour and Pahurehure Inlet. A latitude/longitude grid was used, with 225 longitude cells from 174.5°E to 174.948°E, and 155 latitude cells from 36.92°S to 37.23°S. The spectral grid had 32 discrete frequencies logarithmically placed between 0.10 Hz and 2.00 Hz, and 24 direction bins at 15° increments. All other model settings were SWAN defaults as described in the manual (Holthuijsen et al. 2000).

4.6   SWAN Wave Model Description

The SWAN model (Booij et al. 1999; Ris et al. 1999) is a spectral wave model particularly intended for shallow-water applications in coastal and estuarine environments. It describes the sea state at each time (t) and position (x, y) within a defined region in terms of the amount of energy associated with each wave frequency (f) and propagation direction (θ). The model computes the evolution of the wave spectrum $F(f,\theta)$ by accounting for the input, transfer and loss of energy through various physical processes. These processes include:

- wave generation by wind stress;

- wave propagation;

- refraction by the seabed and/or currents;

- transfer of energy between interacting waves of different frequencies and directions (a nonlinear effect);

- dissipation by white-capping;

- depth-induced breaking;

- bottom friction.

The model takes inputs specifying relevant environmental conditions, including:

- wind speed and direction;

- water depth;

- current speed and direction;

- incident wave conditions at the domain boundary.

In the most general case, the above parameters can be given as a function of position (x, y) and time (t), although sometimes a "stationary" simulation is done, where the equilibrium sea state is computed assuming time-invariant conditions.

4.7   Calibration simulations

The SWAN model was first applied in a non-stationary (time-varying) simulations corresponding to the DP1 and DP2 field programs. Each simulation used water levels and currents, varying in space and time from a calibrated MIKE3 FM HD simulation. Time-varying, spatially constant wind fields were derived from data recorded at Auckland Airport as shown in Figure 11a and 11b. No wave boundary conditions were applied.

4.7.1   Comparison with measurements

Wave statistics for direct comparison to SWAN model predictions during the two observational periods were provided by the DOBIE wave-recording pressure sensors.

Southeastern Manukau Harbour/Pahurehure Inlet Contaminant Study:
Hydrodynamic wave and sediment transport model implementation and calibration

38

Pressure time series from the DOBIEs were used to compute estimates of statistics including significant wave height, mean water depth, peak and mean wave period, and root-mean-square bed orbital velocity. The methodology is described more fully in Appendix 3. These values were then compared with the corresponding statistical output from the SWAN simulations at the corresponding mooring locations.

Results from the final calibration run were plotted against DOBIE data obtained from sites D1, D2, D3, D4 and D9 for a two day period starting on 15 February 2007 (Year day 45) in Figures 13 to Figure 17.

The figures generally illustrate reasonable agreement between observed, MIKE3 FM HD/DOBIE mooring depth records and the predicted water depths produced by the SWAN model simulations. The model-data discrepancies between the simulated and measured mean water levels relate to some slight difference in the actual depths recorded at the DOBIE sites and the interpolated depth values used in the SWAN grid. The SWAN model used a 100 m regular grid which was produced from the MIKE3 FM mesh. Therefore, some specific localised sub-grid scale details could have been lost in the process. However, the SWAN model is only weakly dependent on depth above a certain threshold as the model calculates the wave spectra at the sea surface.

Appendix 3 explains how a high-frequency cutoff is used in computing wave statistics from pressure data. Typically, values of about 1 Hz would be appropriate for 1 m water depth, and about 0.5 Hz for 3 m water depth, representative of the depth ranges at the DOBIE measurement sites. The estimation of mean period from the spectral moments is particularly sensitive to the higher-frequency range of the spectrum, and applying a cut-off can significantly increase the estimated mean periods.

Therefore, it can be expected that the results for the observed significant wave height (Hs) at the DOBIE sites are in good agreement with the SWAN simulations. However, at 2-3 m depth, typical of high tide records, the mean periods estimated from DOBIE data are about 2-3 seconds, corresponding to frequencies of 0.5 Hz which are close to the attenuation limit. Experience has shown that in reality the SWAN model will produce more realistic wave period predictions than the DOBIE PT that tends to over predict wave period at these depths.

Southeastern Manukau Harbour/Pahurehure Inlet Contaminant Study:
Hydrodynamic wave and sediment transport model implementation and calibration

39

Figure 13:

Comparison of data recorded by DOBIE wave recorder at site D1 (+) with output for the same location from the SWAN simulation (black lines). From top to bottom: significant wave height (Hsig), peak wave period (Tpeak), mean (dotted line: first moment, solid line: second moment) wave period, mean depth (Hmean). This simulation runs from 00:00NZST on 15 February 2007 (time = 45 days) to 00:00 NZST on 18 February 2007 (time = 47 days).

Manukau200ZA.out Dobie 01
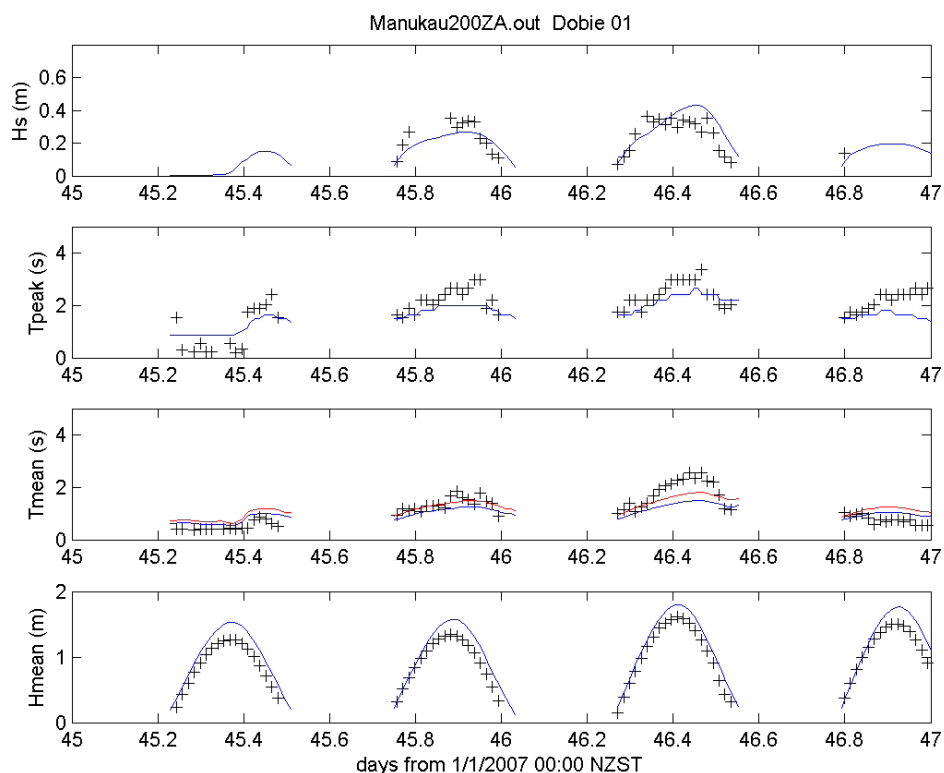
Figure 14:

Comparison of data recorded by DOBIE wave recorder at site D2 (+) with output for the same location from the SWAN simulation (black lines). From top to bottom: significant wave height (Hsig), peak wave period (Tpeak), mean (dotted line: first moment, solid line: second moment) wave period, mean depth (Hmean). This simulation runs from 00:00NZST on 15 February 2007 (time = 45 days) to 00:00 NZST on 18 February 2007 (time = 47 days).

Manukau200ZA.out Dobie 02

Southeastern Manukau Harbour/Pahurehure Inlet Contaminant Study:
Hydrodynamic wave and sediment transport model implementation and calibration
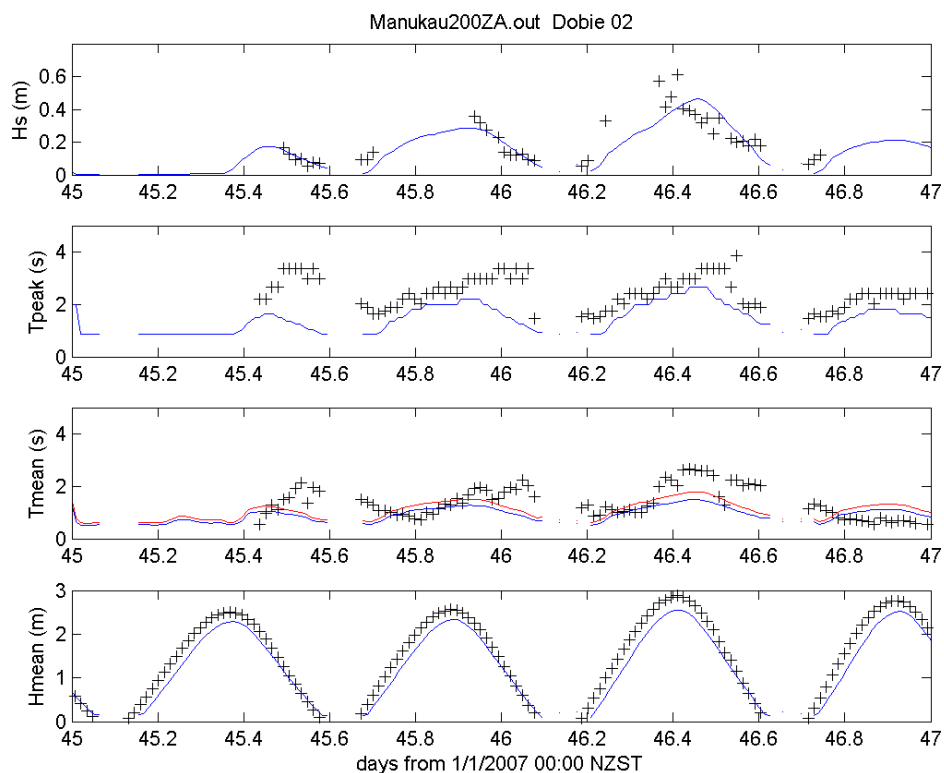
41

Figure 15:

Comparison of data recorded by DOBIE wave recorder at site D3 (+) with output for the same location from the SWAN simulation (black lines). From top to bottom: significant wave height (Hsig), peak wave period (Tpeak), mean (dotted line: first moment, solid line: second moment) wave period, mean depth (Hmean). This simulation runs from 00:00NZST on 15 February 2007 (time = 45 days) to 00:00 NZST on 18 February 2007 (time = 47 days).
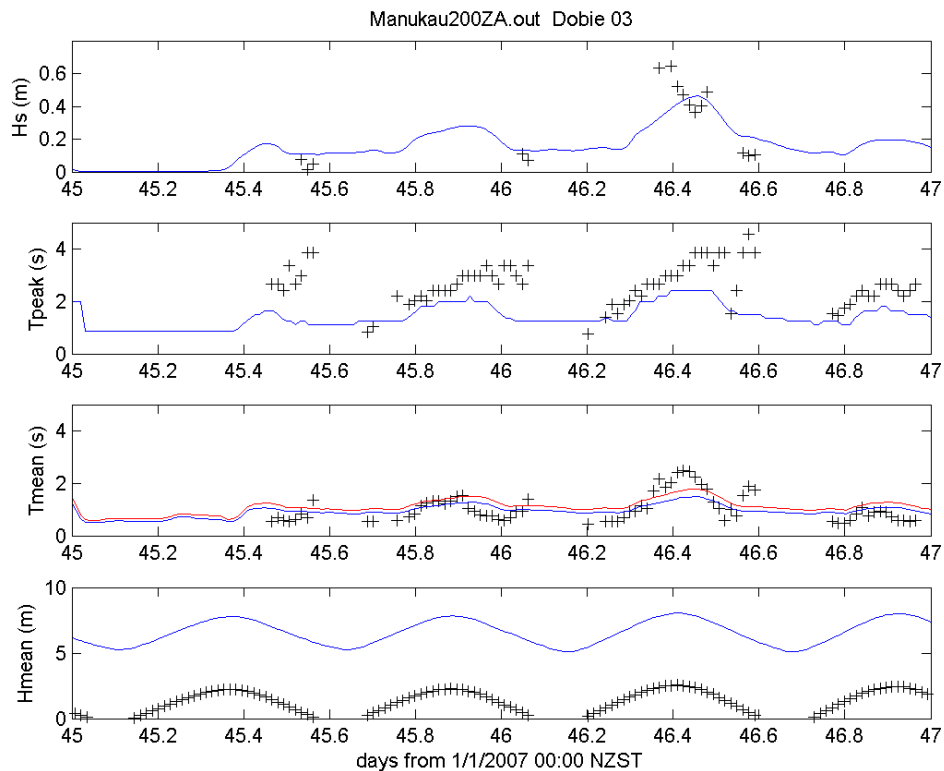
Figure 16:

Comparison of data recorded by DOBIE wave recorder at site D14(+) with output for the same location from the SWAN simulation (black lines). From top to bottom: significant wave height (Hsig), peak wave period (Tpeak), mean (dotted line: first moment, solid line: second moment) wave period, mean depth (Hmean). This simulation runs from 00:00NZST on 15 February 2007 (time = 45 days) to 00:00 NZST on 18 February 2007 (time = 47 days).

Southeastern Manukau Harbour/Pahurehure Inlet Contaminant Study:
Hydrodynamic wave and sediment transport model implementation and calibration
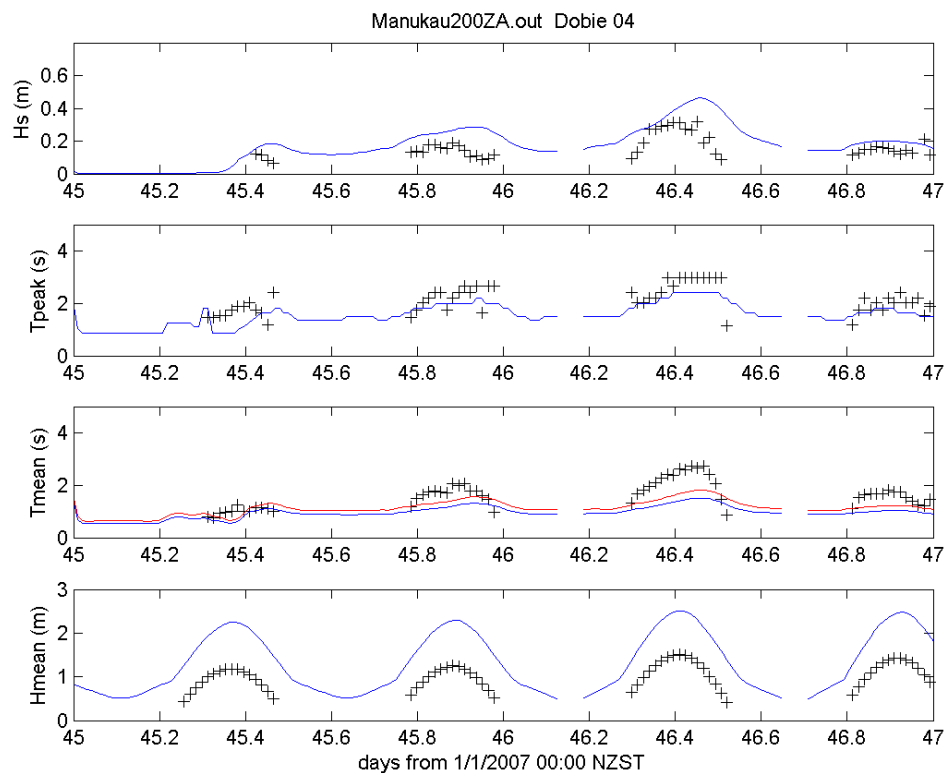
43

Figure 17:

Comparison of data recorded by DOBIE wave recorder at site D9 (+) with output for the same location from the SWAN simulation (black lines). From top to bottom: significant wave height (Hsig), peak wave period (Tpeak), mean (dotted line: first moment, solid line: second moment) wave period, mean depth (Hmean). This simulation runs from 00:00NZST on 15 February 2007 (time = 45 days) to 00:00 NZST on 18 February 2007 (time =47days).
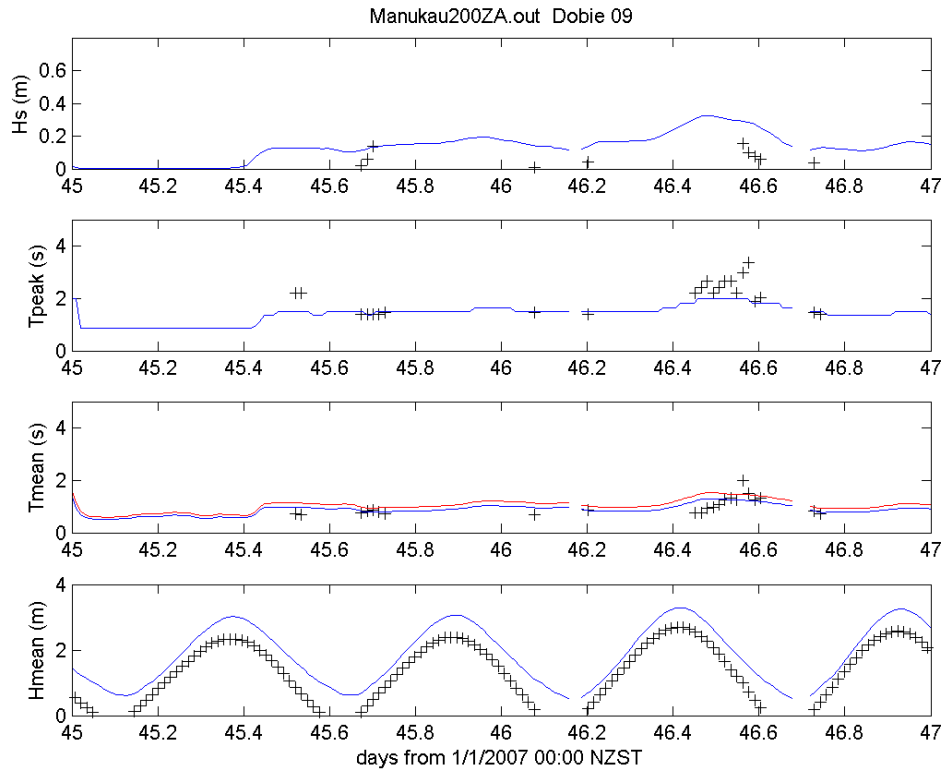

4.8   Suspended Sediment Concentration

The final step in the calibration process was to compare the MIKE3 FM MT sediment transport model against measured suspended sediment concentrations (SSC).

The SSC measurements, as described in detail by Pritchard et al. (2008), were made between 30 – 80 cm above the bed using optical backscatter sensors (OBS) attached to moored DOBIE positioned in the harbour and inlet as shown in Figure 6a. Each OBS sensor was calibrated against sediment samples collected during instrument deployment/recovery.

The two calibration periods were as those used for the MIKE3 FM HD and SWAN models:

- The first during DP1 had relatively small freshwater/sediment inputs at all sources with the exception of one major rainfall event of approximately 58 mm. Winds were directed from the SW and varied in magnitude from approximately 2 m s^{-1} and peaked at about 10 m s^{-1}.

- The second calibration during DP2 again was subject to extended periods of no rainfall and only one or two days when approximately 20 mm rain was recorded. Wind speeds during DP2 were in the range of 4-8 m s^{-1} and from a constant south-westerly direction.

The particle sizes of 4, 12 and 40 μm used in the Southeastern Manukau sediment transport model differs in size orders as compared to that used in the Central Waitemata Harbour (CWH) study (Swales et al. 2007). This decision to reduce particles sizes to 4, 12 and 40 μm was based on the recent analysis of contaminated surface sediment concentration in the Southeastern Manukau by Reed et al. (2008). In the Southeastern Manukau and Pahurehure Inlet, their analysis suggests the highest present day and historic median concentrations of copper (Cu) and zinc (Zn) are associated with particle sizes <25 μm (mud). The next highest level of heavy metal concentrations was associated with the 25-62.5 μm range. The heavy metal concentrations on larger sand size particles >63 μm were not much above background levels in the Pahurehure Inlet. Furthermore studies by for example, Green and Coco (2007) indicate that sediment coarser than fine sand is not likely to be mobilised in any significant way by waves and currents in enclosed harbours. Hence, any sediment coarser than fine sand is considered here to be "relict", and does not contribute to the suspended-sediment load.

Based on the chosen size distribution, the Stokes fall speed assuming sediment density of 2,650 kg m^{-3} (quartz) was assigned to each grainsize: 0.00001 m s^{-1}, 0.0001 m s^{-1} and 0.001 m s^{-1}, respectively, for the 4, 12 and 40 μm fractions. Because the Stokes fall speed is assigned on the assumption of quartz density, the 4, 12 and 40 μm particles are assumed to be in an unaggregated state.

Unaggregated sediment particles are used in the model because (1) mud content of harbour bed sediment is typically <10% by volume – the clay and silt fractions were the most numerous over the Southeastern Manukau Harbour (Reed et al. 2008); (2) the harbour is relatively open and energetic, which will tend to promote the breakup of aggregates, and (3) suspended-sediment concentrations are typically too low (generally <100 mg l^{-1}; rarely exceeding 200 mg l^{-1}) to promote aggregation.

We examine later the applicability of the sediment-transport equations in the MIKE3 FM MT model to the 4, 12 and 40 μm grainsizes.

As with the salinity calibration, the daily freshwater inflow from each of the catchment outlets was derived by applying the TP108 approach (ARC, 1999) to daily rainfall data. Background (baseline) sediment input was arrived at from mean SSC levels during no rain conditions from DOBIE data in Glassons (D7) and Drury Creek (D10), two of the major inputs of freshwater and sediments into the Pahurehure Inlet. These baseline SSC values for the two creeks were also compared to SSC values measured in the Pahurehure Inlet channels (D8 and D11) and all were in a close range of agreement (<50 mg l^{-1}).

During the two instrument deployment periods, rainfall with the exception of two short lived events was low. Consequently, the source freshwater discharge and associated SSC inputs to the inlet were also reduced to background levels in the creeks. In

addition, wind wave activity inside the inlet and creeks is restricted through reduced fetch.

Hence, as shown in Figures 19a and 19b through the observed SSC concentrations measured at four sub-tidal sites, tidal processes dominated sediment transport. The figures show a clear dominant semi-diurnal and spring-neap tidal signal in the observed SSC at all four of the sub-tidal DOBIE sites.

The sediment transport model calibration process for the SEM harbour followed a similar approach to that of the CWH harbour study (Oldman et al. 2007). For the starting point of the MT calibration process, literature recommended values were used for the initial model spin up. The critical bed shear stress for erosion τ_{ce} is suggested to be set for cohesive type sediments at 0.15 N m^{-2} for freshly deposited sediments (Whitehouse et al. 2000). Therefore, the initial τ_{ce} for the whole of the model domain was set to 0.15 N m^{-2}. The critical bed shear stress for deposition was set at $\tau_{cd} = \tau_{ce}$ as a start point for each of the three sediment grainsizes.

The MIKE3 FM MT model was then spun up (ran until stable) for the 14 days that preceded each calibration period using mean freshwater inflow rates and associated sediment inputs computed from TP108 and the DOBIE data. The hydrodynamic and sediment parameters provided by the model spin up were then used to initiate the two main model calibration runs.

The next stage of the calibration process compared modelled and observed SSC at several of the sub-tidal DOBIE sites. This involved an iterative process of adjusting α, the erosion coefficient and E_l, the power of erosion in the sediment model until a satisfactory level of fit was achieved between measured and predicted SSC. E_1 in context of the Southeastern Manukau model calibration was the approximate base line erosion rate during neap tides. The α exponent coefficient was used to parameterise the erosion rate through an increasing range of excess bed shear. This becomes especially important during spring tides as the bed shear stress increases due to an increase in the magnitude of tidal currents.

Figure 18:

Comparison of published erosion rates and the erosion rate for the MIKE3 FM MT model calibrated for the Southeastern Manukau Harbour and Pahurehure Inlet.
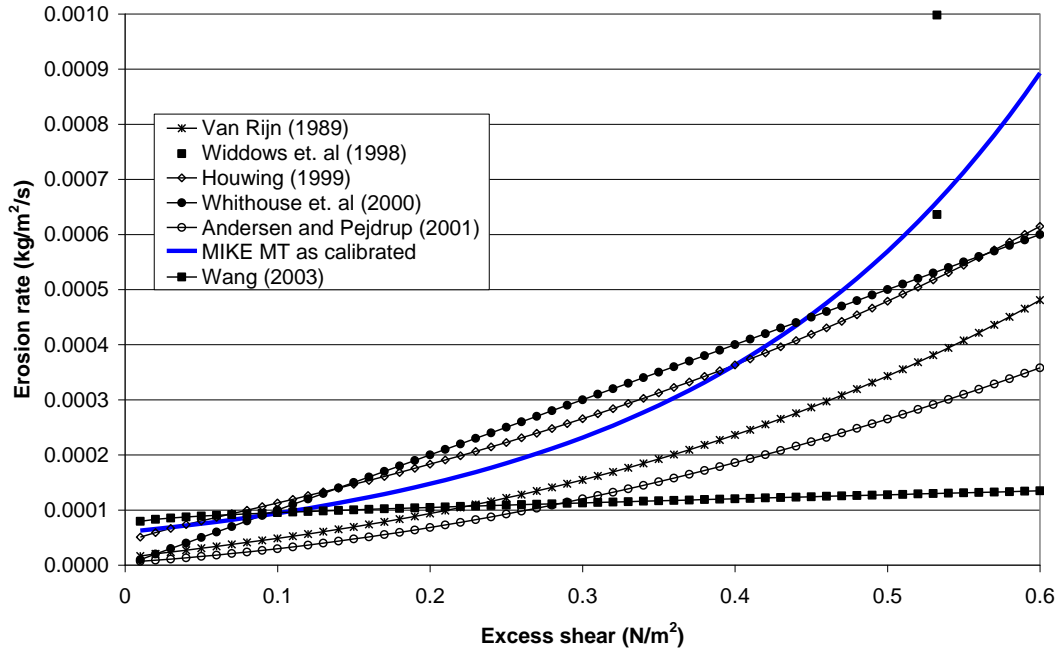
After consecutively tweaking model α and E_l the general best fits to the observed data over the two deployment/calibration periods were $E_l = 0.00006$ kg.m^{-2}s^{-1} and $\alpha =$ 4.5 for $(\tau_b - \tau_{ce})$ <0.45 N m^{-2}. The erosion rate using these values falls within the range of published rates (Van Rijn, 1989; Widdows et. al, 1998; Houwing, 1999; Whitehouse, 2000; Andersen and Pejrup, 2001; Wang, 2003) for similar physical settings and grainsizes. Figure 18 shows that the calibrated erosion rate begins to diverge from published rates for higher values of $(\tau_b - \tau_{ce})$. Using higher values of E_l caused the model to over predict SSC during neap tides. Further increasing values of α caused the model to over predict SSC during spring tides.

The next stage of the calibration adjusted τ_{cd}, the critical shear stress for deposition for any fine suspended sediments in the 4 and 12 µm range. After a series of trials the best agreement between observed and predicted SSC was by using τ_{cd} values of 0.07 N m^{-2} and 0.1 N m^{-2} for the 4 and 12 µm particles respectively. Lowering τ_{cd} for the larger 40 µm fraction caused the model to over predict the peak levels of sediment re-suspension through the tidal cycle.

As a final check of the calibration process, the 14 day spin-up period was rerun using all of the calibration values determined from the model runs, which provided another initial condition for the SSC and grain size composition of the bed sediment. The calibrated model, together with these new initial conditions, was then used to predict SSC for the calibration periods.

Results from the two calibration (instrument deployment) periods are illustrated in Figure 19a and Figure 19b through a series of time series inter-comparisons between

modelled and observed SSC at each of the four sub-tidal DOBIE sites. Figure 20a-20b and Table 4 further shows these results in context of a linear regression between observed and predicted SSC at each sub-tidal DOBIE Mooring site.

The observed data in the two tidal creeks (D7 and D10) shows the dominance of the semi-diurnal and fortnightly period tidal signal that modulates the SSC signal. Despite the two rainfall events during the deployments, SSC concentrations for these sites remained low and seldom exceeded maximums of 100 mg l^{-1}. The phase modulation of SSC in the observed and modelled data is in close agreement at semi-diurnal frequencies. Here the model simulates the main peaks and troughs in SSC through consecutive semi-diurnal tidal excursions and also through the spring-neap cycle according to rising water depths and increasing bed shear stress.

The DOBIE SSC measurements collected at the more exposed mid channel inlet sites at D8 and D11 show far more variation in the SSC signal. During DP2 (DOBIE D8 SSC produced spurious results during DP1) the modelled and observed SSC at D8 was in reasonable agreement. During slightly higher wind speeds (8-10 m s^{-1}) as observed for a short period during DP1 (year day 73-75), the observed and modelled SSC still showed close agreement. The observations seemingly only detected a relatively small change in SSC. This as previously mentioned was probably caused by the inlet sub-tidal mooring sites being largely in the lee of the dominant SW winds.

The phase relationship between the observed and predicted SSC through both deployment periods was in excellent agreement. The general trend of the MT models performance was to slightly over predict SSC during DP1 and under predict SSC during DP2.

However, as shown in Figures 19a and 19b the magnitudes of SSC were not always predicted correctly. This aside, the general trend for higher SSC during strong spring tidal flows and lower SSC during weaker neap tidal flows was both observed and simulated. Calibration above 100 mg l^{-1} was not possible as during the deployments no high SSC was observed at any of the sub-tidal sites. Therefore, the absence of high SSC likely decreases the quality of the R^2 fits shown in Table 4.

Table 4:

Results from the linear regression between predicted (x) and measured (y) suspended sediment concentrations plus R^t values for sub-tidal DOBIE sites D7, D8, D10, and D11. Results are shown for the combined DP1 and DP2 calibration periods.

Site	Linear regression for DP1	R^2
D7	y = 0.6x + 4.7	0.5
D8	y = 0.7x - 2.3	0.5
D10	y = 0.6x + 5.4	0.4
D11	y = 0.8x -1.8	0.4

4.9   Summary

The observed and modelled sea surface elevation phase relationship in the model domain was in good agreement. However, there was some disparity between absolute amplitudes. This was probably caused by the localised non-resolved variations in bed roughness and bathymetry in the model. Nevertheless, overall the amplitude error was small as compared to the total amplitude of the tide at all of the five measured sites.

The predicted current at the open water sites in the harbour showed a good general agreement in phase with the model. Phase and ellipse properties for major semi-diurnal forcing constituents were in reasonable agreement with those measured by the current meters. Nevertheless, up to 34% difference was observed between observed and modelled current amplitudes. This was not directed to a specific bias i.e., observed or modelled. Therefore, we assume this is product of variations in the real and modelled bathymetry which causes the variation in the currents.

Two of largest discrepancies between the observations and the model were in Glassons and Drury Creek (Figure 9c and 9d). These narrow tidal creeks that lead into the Pahurehure Inlet had a complex bathymetry with many meanders and changes in roughness (boulders to scoured bottom). With a compromise between computation time, element numbers and model stability, these small scale features were not possible to resolve with a regional scale model scheme. This aside, the model produced the correct trends and the correct order of magnitude in the current forcing.

Low rainfall through the two field studies seriously hampered the salinity calibrations. Source inflow rates were mostly limited to baseline conditions. As with the tides, phase changes in the observed and modelled salinity were in good agreement. These oscillations were especially evident in Glassons and Drury Creek, where the majority of fresh/brackish water is discharged into the Pahurehure Inlet. Despite this, the amplitude of the salinity change was generally under predicted. This was a possible result of underestimating freshwater inflow from the TP108 approach, discrepancy in bed roughness and bathymetry and the bulk approach (element scale) to parameterising turbulence and mixing.

The SWAN model of the region driven by the MIKE3 FM HD model and localised wind fields produced wave heights comparable to the DOBIE observations. Water depths predicted by SWAN were overall in close agreement with the MIKE3 FM HD and DOBIE measurements.

Suspended sediment transport (SSC) was strongly linked to tidal flows during the study period. SSC peaked during ebb and flood and dropped off during slack tide. SSC magnitudes also showed a strong spring–neap tidal signature, with SSC magnitudes rising to their largest values at spring tide and their lowest values at ebb tide. Occasional spikes in SSC were also observed due to processes unrelated to tidal flows.

The model represented the main (tidally driven) sediment transport processes. It correctly represented the timing of SSC peaks associated with peak tidal flows and also reproduced the spring–ebb tidal modulation. This is despite the significant difficulties associated with predicting cohesive sediment transport.

It was unfortunate that the timing of the field study did not coincide with any large rainfall events nor any large riverine inputs of suspended sediments. Therefore, the models were not tested in their capacity to represent a high SSC concentration plume entering from tidal creeks. However, the representation of tidal-induced sediment transport suggests that the subsequent dispersion of riverine sediment pulses by the tides is likely to be well represented.

Figure 19a:

Observed and modelled suspended sediment concentration (SSC) at four sub-tidal DOBIE sites (see Figure 1) for deployment 1 (DP1) between 15ᵗʰ February 2007-26ᵗʰ March 2007.

Southeastern Manukau Harbour/Pahurehure Inlet Contaminant Study:
Hydrodynamic wave and sediment transport model implementation and calibration

51
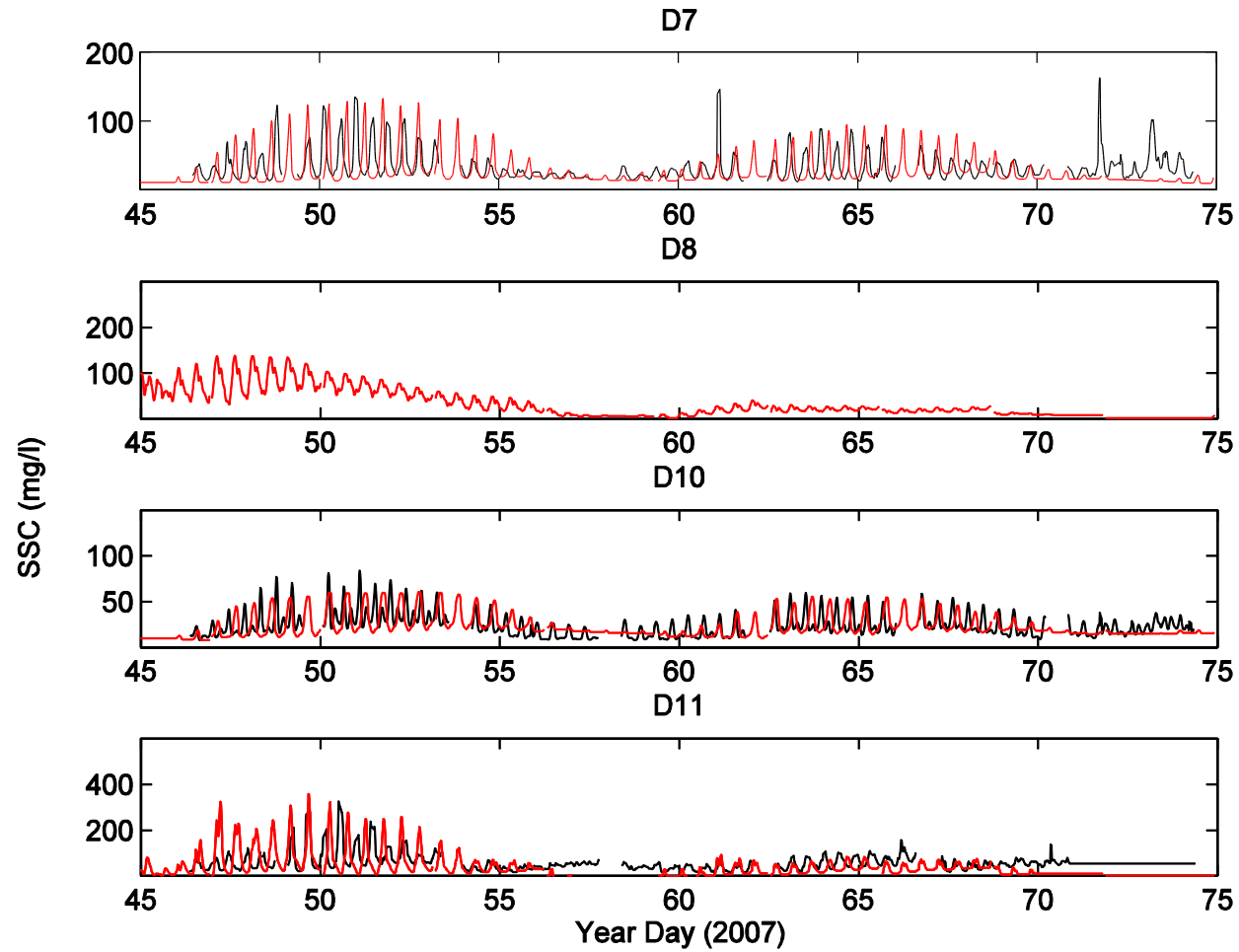
Figure 19b:

Observed and modelled suspended sediment concentration (SSC) at four sub-tidal DOBIE sites (see Figure 1) for deployment 1 (DP2) between 24ᵗ April 2007-29ᵗ May 2007.

Southeastern Manukau Harbour/Pahurehure Inlet Contaminant Study:
Hydrodynamic wave and sediment transport model implementation and calibration

52

Figure 20a:

Observed versus modelled suspended sediment concentration (SSC) at four sub-tidal DOBIE sites (see Figure 1) for deployment 1 (DP1) between 15th February 2007-26th March 2007.
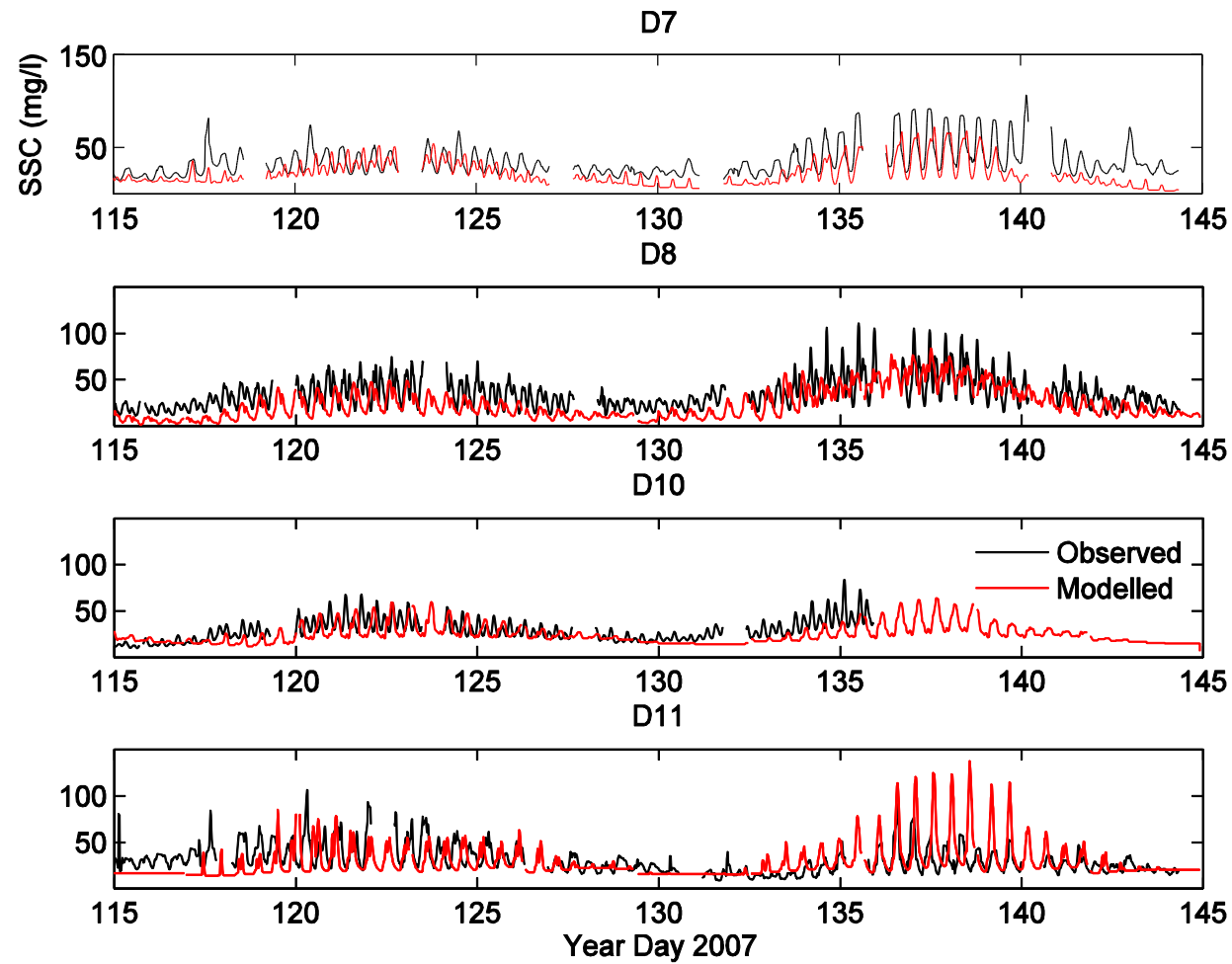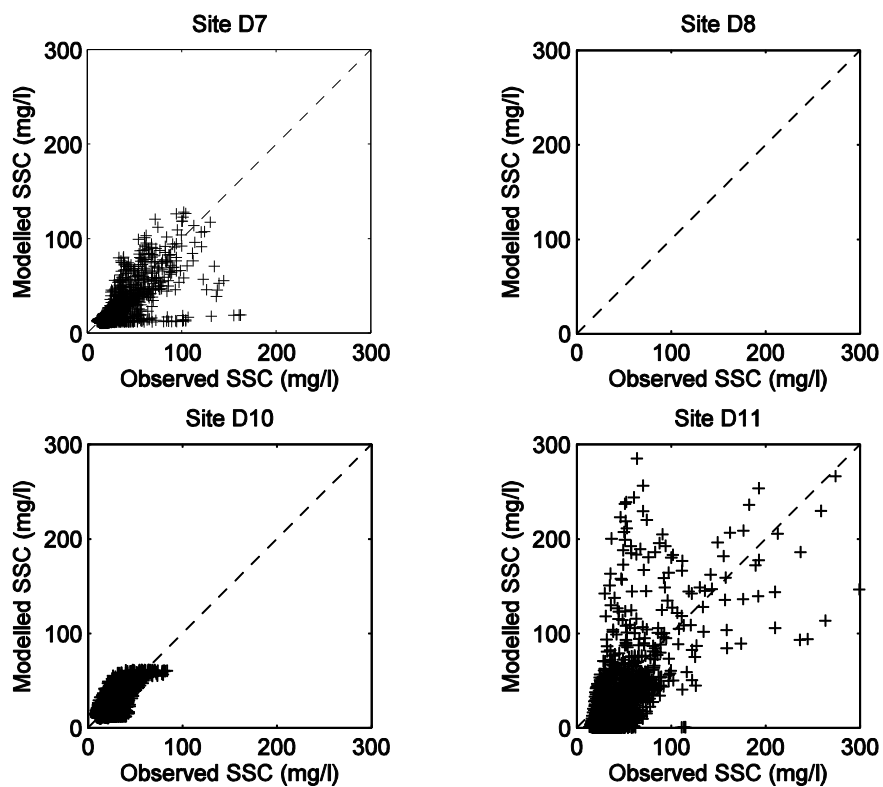
Figure 20b:

Observed versus modelled suspended sediment concentration (SSC) at four sub-tidal DOBIE sites (see Figure 1) for deployment 1 (DP2) between 24 April 2007-29 May 2007.

Southeastern Manukau Harbour/Pahurehure Inlet Contaminant Study:
Hydrodynamic wave and sediment transport model implementation and calibration

54

Southeastern Manukau Harbour/Pahurehure Inlet Contaminant Study:
Hydrodynamic wave and sediment transport model implementation and calibration

55
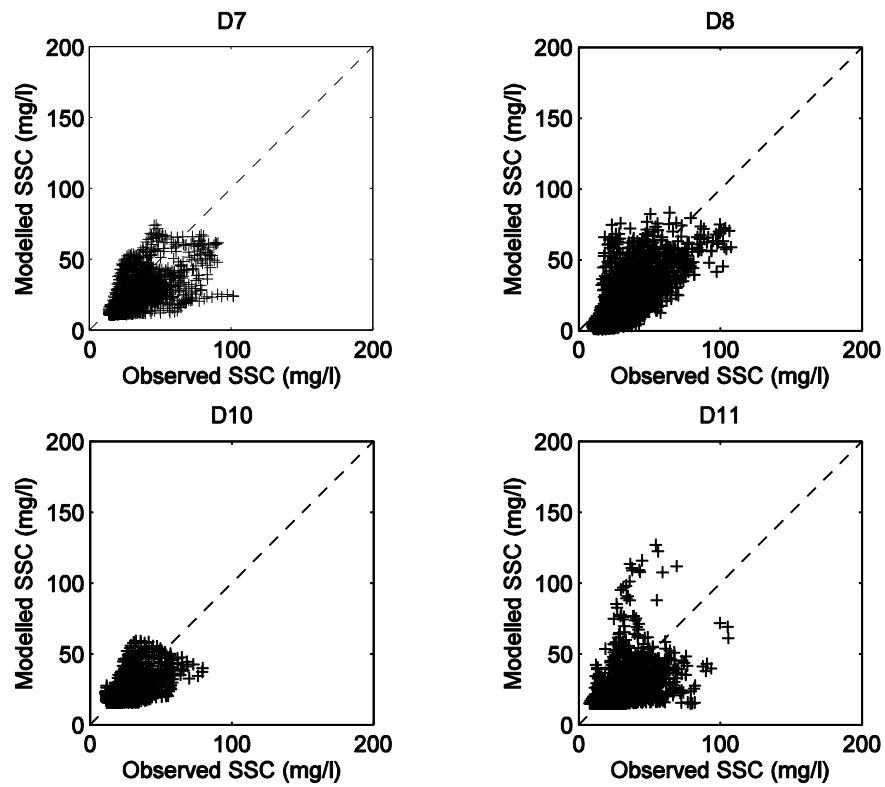
5 References

Andersen, T.J.; Pejrup, M. (2001). Suspended sediment transport on a temperate, microtidal mudflat, the Danish Wadden Sea. *Marine Geology 173*: pp. 69-85.

Auckland Regional Council (1999). Guidelines for stormwater runoff modelling in the Auckland Region, Auckland Regional Council, Technical Publication No. 108, April 1999, ISSN 1172-6415.

Bell, R., Dumnov, S., Williams, B. and Greig, M. 1998. Hydrodynamics of Manukau Harbour, New Zealand. New Zealand Journal of Marine and Freshwater Research, 32: 81-100.

Booij, N.; Ris, R.C.; Holthuijsen, L.H. (1999). A third generation model for coastal regions. Part I: Model description and validation, *Journal of Geophysical Research, Vol. 104*, No. C4, pp. 7649-7666.

Emery, W.J.; Thomson, R.E. (2001). Data Analysis Methods in Physical Oceanography. Elsevier, Amsterdam, Netherlands.

Fredsøe, J. (1984). Turbulent boundary layer in wave-current motion. *Journal of Hydrological Engineering, A.S.C.E, Volume 110*, HY8, 1103-1120 (1984).

Green, M.O.; Coco, G. (2007). Sediment transport on an estuarine intertidal flat: measurements and conceptual model of waves, rainfall and exchanges with a tidal creek. *Estuarine, Coastal and Shelf Science 72*: 553-569.

Holthuijsen, L.H.; Booij, N.; Ris, R.C. (1993). A spectral wave model for the coastal zone, Proceedings of 2nd International Symposium on Ocean Wave Measurement and Analysis, New Orleans, USA, pp. 630–641.

Holthuijsen, L.H.; Booij, N.; Ris, R.C.; Haagsma, I.G.; Kieftenburg, A.T.M.M.; Kriezi, E.E. (2000). SWAN Cycle 3 version 40.11 user manual. Delft University of Technology.

Houwing, E.J. (1999). Determination of the critical erosion threshold of cohesive sediments on intertidal mudflats along the Dutch Wadden Sea Coast. *Estuarine, Coastal and Shelf Science 49*: pp. 545–555.

Oldman, J.; Gorman, R.; Lewis, M. (2007). Central Waitemata Harbour Contaminant Study. Harbour Hydrodynamics and Sediment-Transport Model Implementation and Calibration. NIWA Client Report HAM-2007-102. Prepared for Auckland Regional Council.

Southeastern Manukau Harbour/Pahurehure Inlet Contaminant Study:
Hydrodynamic wave and sediment transport model implementation and calibration

56

Pawlowicz, R.; Beardsley, B. & Lentz, S. (2002). Classical tidal harmonic analysis including error estimates in MATLAB using T_TIDE". *Computers and Geosciences 28*: 929-937.

Pritchard, M.; Hancock, N.; Lewis, M. (2008). Southeastern Manukau and Pahurehure Inlet Contaminant Study: Harbour Hydrodynamics and Sediment Transport Fieldwork. Auckland Regional Council Technical Report TR2008/055

Reed, J.; Swales, A.; Ovenden, R.; Buckthought, D.; Rush, N.; Wadhwa, S.; Okey, M.J. (2008). South East Manukau Harbour Study: Harbour Sediments. Auckland Regional Council Technical Report TR2008/054

Ris, R.C.; Booij; N.; Holthuijsen, L.H. (1999). A third-generation wave model for coastal regions. Part II: Verification, *Journal of Geophysical Research, Vol. 104*, No. C4, pp. 7667-7682.

Soulsby, R.L.; Hamm, L.; Klopman, G.; Myrhaug, D.; Simons, R.R.; Thomas, G.P. (1993). Wave-current interaction within and outside the bottom boundary layer *Coastal Engineering 21*: 41-69 (1993).

Swales, A.; Stephens, S.; Hewitt, J.; Ovenden, R.; Hailes, S.; Lohrer, D.; Hermansphan, N.; Hart, C.; Budd, R.; Wadhwa, S.; Okey, M. (2007). Central Waitemata Harbour Study. Harbour Sediments. Auckland Regional Council Technical Report TR2008/034

Swart, D.H. (1974). Offshore sediment transport and equilibrium beach profiles. Delft Hydraulic Laboratory Publication 1312, Delft University of Technology, The Netherlands.

Van Rijn, L.C. (1989). Handbook on Sediment Transport by Current and Waves. *Delft Hydraulics*, Report H461, pp. 12.1-12.27.

Walters, R.A.; Goring, D.G., Bell, R.G. (2001). Ocean tides around New Zealand. *New Zealand Journal of Marine and Freshwater Research 35*: 567-579.

Wang, Y.H. (2003). The intertidal erosion rate of cohesive sediment: a case study from Long Island Sound. *Estuarine, Coastal and Shelf Science 56*: pp. 891–896.

Whitehouse, R.; Soulsby, R.; Roberts, W.; Mitchener, H. (2000). Dynamics of estuarine muds. Thomas Telford.

Widdows, J.; Brinsley, M.D.; Bowley, N.; Barrett, C. (1998). A Benthic Annular Flume for In Situ Measurement of Suspension Feeding/Biodeposition Rates and Erosion Potential of Intertidal Cohesive Sediments. *Estuarine, Coastal and Shelf Science 46*: pp. 27–38.

Southeastern Manukau Harbour/Pahurehure Inlet Contaminant Study:
Hydrodynamic wave and sediment transport model implementation and calibration

57

6 Appendix 1: LIDAR Data Processing

The LIDAR data were supplied to NIWA in a raster (*.las) format, which once imported into LASEdit software can be viewed, post processed and output into an *.xyz (ascii readable format). These data were then converted from NZTM, corrected to local chart datum and converted to WGS84 co-ordinates and saved in a binary Matlab format for further post processing.

Several hundred binary files were then put through a data reduction routine to make the size of data importable to the DHI MIKE ZERO grid generation tool. Each data file (tile) was concatenated and interpolated onto a regular grid of a sub-region of the area. Then each sub-region was again concatenated again and interpolated onto a regular grid of the whole region. In this way LIDAR bathymetry can easily be reprocessed using Matlab files if higher/lower spatial resolution is required.

7 Appendix 2: Formulation of processes simulated by the MIKE3 models

This section outlines the methods used by the MIKE3 FM HD and MT models to simulate tidal propagation within the harbour, tide- and wind-driven currents, freshwater mixing and sediment transport.

7.1 Bed shear stress

MIKE3 FM HD uses a quadratic friction law to define the bed shear stress due to the current:

$$\frac{\overline{\tau}_b}{\rho_0} = c_f \overline{u}_b |\overline{u}_b|$$

where c_f is the drag coefficient, $\overline{u}_b$ is the time-averaged current speed at a distance Δz_b above the bed, and ρ_0 is the density of water. The drag coefficient is defined in terms of a logarithmic profile between the seabed and the point Δz_b above the seabed:

$$c_f = 1 \frac{1}{\left(\frac{1}{\kappa} \ln\left(\frac{\Delta z_b}{z_0} \right) \right)^2}$$

where $\kappa = 0.4$ is von Karman's constant and z_0 is the bed roughness length, which is typically varied to calibrate the model.

The enhancement of the current-related bed shear stress by any waves that may be present is increased for use in the calculation of sediment transport. The method used is a parameterisation of Fredsøe's (1984) method, which was derived by Soulsby et al. (1993). The mean and maximum combined wave-current bed shear stresses are given as follows:

$$\frac{\tau_{wc,mean}}{\tau_c + \tau_w} = \frac{\tau_c}{\tau_c + \tau_w} \left(1 + b \left(\frac{\tau_c}{\tau_c + \tau_w} \right)^p \left(1 - \frac{\tau_c}{\tau_c + \tau_w} \right)^q \right)$$

Southeastern Manukau Harbour/Pahurehure Inlet Contaminant Study:
Hydrodynamic wave and sediment transport model implementation and calibration

59

$$\frac{\tau_{wc,max}}{\tau_c + \tau_w} = \left(\frac{\tau_c}{\tau_c + \tau_w}\right)^m \left(1 - \frac{\tau_c}{\tau_c + \tau_w}\right)^n$$

where *b, p, q, a, m, n* constants:

a=a1 + a2 cosγ i +(q3 + q4 cosγ i)log10(r)
b=b1 + b2 cosγ j +(b3 + b4 cosγ j)log10(r)
m=m1 + m2 cosγ i +(m3 + m4 cosγ i)log10(r)
n=n1 + n2 cosγ i +(n3 + n4 cosγ i)log10(r)
p = p1 + p2 cosγ j +(p3 + p4 cosγ j)log10(r)
q=q1 + q2 cosγ j +(q3 + q4 cosγ j)log10(r)

and *a1, a2*, etc. are given in the table below, γ is the angle between the waves and currents with *I* = 0.8, *j* = 3.0 and *r* = 2 f_w/f_c.

	a	m	n	b	p	q
1	-0.06	0.67	0.75	0.29	-0.77	0.91
2	1.70	-0.29	-0.27	0.55	0.10	0.25
3	-0.29	0.09	0.11	-0.10	0.27	0.50
4	0.29	0.42	-0.02	-0.14	0.14	0.45

f_w is the pure-wave wave friction factor, given by (Swart, 1974) as:

$$f_w = \exp\left(5.213\left(\frac{a}{k}\right)^{-0.194} - 5.977\right)$$

where *k* is the bed roughness and *a* is the wave-orbital semi-excursion at the bed. Also, f_c is the pure-current friction factor, given by the logarithmic resistance law:

$$f_c = 2\left(2.5\left(\ln\left(\frac{30h}{k}\right) - 1\right)\right)^{-2}$$

where *h* is the water depth.

7.2 Currents

The influence of the wind on currents is treated in terms of the wind-induced shear stress that acts on the sea surface:

$$\tau_w = \rho_a c_d |u_w| \overline{u_w}$$

where ρ_a is the density of air, c_d is the drag coefficient and u_w is the wind speed 10 m above the sea surface. The model is typically calibrated by adjusting c_d.

The turbulent transfer of momentum by eddies gives rise to an internal fluid friction which is resolved in the horizontal and vertical dimensions by use of an eddy viscosity formulation.

In the vertical, the eddy viscosity is derived from the following log-law formulation:

$$v_t = U_\tau h \left(c_1 \frac{z+d}{h} + c_2 \left(\frac{z+d}{h} \right)^2 \right)$$

Here, $U_\tau = \max(U_{\tau s}, U_{\tau b})$, c_1 and c_2 are constants, d is the still-water depth, h is the total water depth, and $U_{\tau s}$ and $U_{\tau b}$ are the friction velocities associated with the surface and seabed shear stresses, respectively. The model is typically calibrated by adjusting the constants c_1 and c_2 and by defining the upper and lower limits of the vertical eddy viscosity.

For the horizontal eddy viscosity, the Smagorinsky formulation was applied, which gives the subgrid-scale eddy viscosity as:

$$A = c_s^2 l^2 \sqrt{2 S_{ij} S_{ij}}$$

where c_s is a constant, l is the characteristic length (approximated by the minimum edge length for each element) and the deformation rate (S_{ij}) is given by

$$S_{ij} = \frac{1}{2} \left(\frac{\partial u_i}{\partial x_j} + \frac{\partial u_j}{\partial x_i} \right)$$

Using this formulation, the model can be calibrated by adjusting the constant c_s and by defining the upper and lower limits of the horizontal eddy viscosity.

7.3   Salinity

In baroclinic mode MIKE3 FM HD requires coefficients for vertical and horizontal dispersion. These can be constant or they can be proportionally scaled to the eddy viscosity. For the implementation of the model here a scaled dispersion coefficient was used.

7.4   Sediment transport

MIKE3 FM MT can simulate the erosion, transport and deposition of up to 8 different grainsize fractions. For each grainsize a fall velocity (w_s) is assigned.

7.4.1 Deposition

Deposition of sediment onto the bed is deemed to occur when and where the bed shear stress (τ_b) is smaller than the critical bed shear stress for deposition (τ_{cd}). A separate τ_{cd} is assigned to each grainsize.

The deposition rate (kg.m^{-2}.s^{-1}) is given separately for each grainsize by:

$$D = w_s \, p_d \, c_b$$

where p_d is the probability ramp function for deposition defined as:

$$p_d = \max(0, \min(1, 1 - \frac{\tau_b}{\tau_{cd}}))$$

and c_b is the near-bed suspended-sediment concentration for the grainsize at hand.

MIKE3 FM MT gives two choices for determining c_b: the Teeter formulation and the Rouse formulation. The Teeter formulation was chosen for implementation here, which is:

$$c_b = \bar{c}\left(1 + \frac{p_e}{1.25 + 4.75 p_d^{2.5}}\right)$$

where p_e is the Peclet number, defined as:

$$p_e = 6 \frac{w_s}{\kappa U_f}$$

and U_f is the friction velocity.

The calibration process involves selecting the fall velocity and the critical bed shear stress for deposition (τ_{cd}) for each grainsize.

7.4.2 Erosion

Erosion of bed material takes place when and where the bed shear stress exceeds the critical shear stress for erosion (τ_{ce}). A single value of τ_{ce} is assigned for the bed sediment as a whole.

The erosion rate (kg/[m^{2}s]) is specified for the bed as a whole as:

$$E = E_I \exp\left(\alpha\left(\tau_b - \tau_{ce}\right)\right)$$

where α is a power term and E_I is the "initial" erosion rate. The total mass of sediment eroded from the bed (which is governed by E) is then distributed amongst the constituent grainsizes by the proportions of the constituent grainsizes in the bed sediment. For example, if constituent grainsize #1 makes up 50% of the bed sediment by mass then 50% of the sediment eroded by E will be assigned that grainsize.

The calibration process involves selecting one value each for τ_{ce}, α and E_I.

Table A2:

List of specific calibration parameters and calibrated as implemented in the DHI MIKE3 FM HD and MT model for the Pahurehure Inlet and Southeastern Manukau Harbour.

DHI MIKE3 FM	Parameter	Variable used in model
Model stability	Model Spin up Time	14 days
Offshore tidal boundary	EZZY tide tidal constituents	M_2, S_2, N_2, K_2, K_1, O_1, P_1, Q_1, $2N_2$, MU_2, NU_2, L_2, T_2
Bed roughness	Z_0	0.1, 0.05
Horizontal Mixing	Smagorinsky coefficient	0.42
Lower limit	$N_{(x,y)}$	1.8e-006 m^2 s^{-1}
Upper limit	$N_{(x,y)}$	10 m^2 s^{-1}
Vertical Mixing	c_1, c_2	0.41, -0.41
Vertical eddy formulation	N_z	1.8e-006 m^2 s^{-1}
Lower limit	N_z	0.4 m^2 s^{-1}
Upper limit		
Salinity scaling factor	S	1.1
Wind drag coefficient	C_d	0.00125
Particle Settling Velocity	4 μm	1e-5 m s^{-1}
	12 μm	1e-4 m s^{-1}
	40μm	1e-3 m s^{-1}
Bed Erosion Rate	E1	6e-5 kg m^{-2} s^{-1}
	α	4.5
Sediment Deposition Threshold	τ_{cd} (4 μm)	0.07 N m^{-2}
	τ_{cd} (12 μm)	0.1 N m^2
	τ_{cd} (40 μm)	0.15 N m^{-2}
Critical Shear Stress for erosion	τ_{cr} (4, 12, 40 μm)	0.15 N m^{-2}

8   Appendix 3: Wave Statistics

Wave data recorded (or computed from a model) at a single point are usually discussed in terms of the variance spectrum $S(f)$ of the sea-surface elevation. The DOBIE, however, does not directly measure the sea-surface elevation, but instead records a time series of pressure, from which a variance spectrum $S_p(f)$ can be obtained. The two spectra are related as:

$$S_p(f) = \rho g\, A(f) S(f)$$

where ρ = 1025 kg.m^{-3} (density of sea water), g = 9.81 m.s^{-2} (gravitational acceleration), and $A(f)$ is a frequency-dependent attenuation function:

$$A(f) = \left(\frac{\cosh(k(z+h))}{\cosh(kh)} \right)^2$$

Here, h is water depth and z is the instrument's vertical elevation above mean water level. The wave number k is related to the frequency f by a dispersion relation:

$$(2\pi f)^2 = gk \tanh(kh)$$

The attenuation function $A(f)$) becomes very small when kh is large, i.e., at frequencies for which the wavelength is much smaller than the water depth. In that case, the part of the high-frequency pressure signal contributed by surface waves becomes small relative to the noise level. To limit the effect of amplification of noise at high frequencies, it is normal to apply a frequency cut-off when estimating $S(f)$.

From the computed spectral energy density $S(f)$, the peak frequency f_p and peak energy $S_p = S(f_p)$ of the spectrum are located. Spectral moments

$$M_j = \int_0^{f_{cut}} f^j S(f) df$$

are computed, allowing further statistics to be defined, including:

❑ significant height $H_s = 4\sqrt{M_0}$

❑ first-moment mean period $T_{m01} = M_0 / M_1$

❑ second-moment mean period $T_{m02} = \sqrt{M_0 / M_2}$

The root-mean-square bed-orbital velocity is calculated as:

$$U_{rms}^2 = \int_0^{f_{cut}} 2\pi f\, A(f) S(f) df$$